IEEE Journal of Microwaves

Received 31 August 2020; revised 18 October 2020; accepted 23 October 2020.
Date of current version 7 January 2021.

Digital Object Identifier 10.1109/JMW.2020.3033992

Microwave and Millimeter Wave Power Beaming

CHRISTOPHER T. RODENBECK [1] (Senior Member, IEEE), PAUL I. JAFFE [1] (Senior Member, IEEE), BERND H. STRASSNER II [2], PAUL E. HAUSGEN [3], JAMES O. McSPADDEN [4] (Senior Member, IEEE), HOOMAN KAZEMI [5] (Senior Member, IEEE), NAOKI SHINOHARA [6] (Senior Member, IEEE), BRIAN B. TIERNEY [1] (Member, IEEE), CHRISTOPHER B. DePUMA [1], AND AMANDA P. SELF [3]

(Invited Paper)

[1]U.S. Naval Research Laboratory, Washington, DC 20375-5307 USA
[2]Sandia National Laboratories, Albuquerque, NM 87185 USA
[3]Air Force Research Laboratory, Kirtland AFB, NM 87117-5776 USA
[4]Raytheon Technologies Corporation, Dallas, TX 75243 USA
[5]Raytheon Technologies Corporation, Thousand Oaks, CA 91361-4443 USA
[6]Research Institute for Sustainable Humanosphere, Kyoto University, Uji 611-0011, Japan

CORRESPONDING AUTHOR: Christopher T. Rodenbeck (e-mail: chris.rodenbeck@ieee.org).

ABSTRACT Power beaming is the efficient point-to-point transfer of electrical energy across free space by a directive electromagnetic beam. This paper clarifies the basic principles of power beaming in simple terms, and proposes a benchmarking methodology for improving the comparative assessment of power beaming systems and technology. An in-depth historical overview tracing the worldwide progress in microwave and millimeter wave (mmWave) experimental demonstrations over the past 60 years shows clear evidence of a significant increase in activity during the last 5 years. In addition, a review of progress in scalable rectenna arrays for the reception of microwave power beaming shows sufficient maturity for new research to initiate on the ruggedization, productization, and system integration aspects of the technology. A review of regulatory issues including spectrum management and safety indicates the need for additional technical solutions and international coordination. Breaking results reported in this paper include 1) data from the first in-orbit flight test of a solar-to-RF "sandwich module", 2) the construction of multiple US in-orbit demonstrations, planned for 2023 launch, that will demonstrate key technologies for space-based solar power, and 3) a 100-kW mmWave power beaming transmitter demonstrating inherent human life safety.

INDEX TERMS Wireless power transmission, microwave power transmission, power beaming, solar power satellites, space solar power, space based solar power, rectennas, rectenna arrays, spectrum management, radiofrequency safety.

I. INTRODUCTION

The recent explosion in commercial applications of wireless power transmission (WPT) necessitates the definition of power beaming [1] as a distinct class of WPT. Stated simply, *power beaming is the efficient point-to-point transfer of electrical energy across free space by a directive electromagnetic beam*. Unlike near-field WPT [2], power beaming utilizes directive, propagating waves. Unlike energy harvesting or passive receiver applications (e.g., radiofrequency identification and internet of things devices, etc.) [3], power beaming has as its primary objective the maximization of total power transfer efficiency—from the DC power generated at the transmitter to the DC power delivered to the load. And unlike directed energy applications [4], the objective of power beaming is the transfer of useful electrical power rather than destructive or disruptive effects.

Power beaming, which originates in the seminal investigations of W. Brown [1], today enjoys an international resurgence of engineering activity. Although a microwave solar power satellite (SPS) for the continuous transfer of boundless electrical power to the Earth remains the most far-reaching application of power beaming technology, smaller-scale use

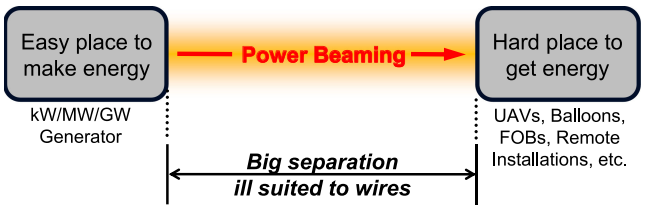

FIGURE 1. **Power beaming functional overview. Example applications include unmanned systems, such as UAVs or balloons, and remote installations, such as forward operating bases (FOBs) or unattended sensors.**

TABLE 1 **Comparison of Power Beaming Modalities**

	Optical	mmWave	Microwave
Penetration clouds/rain/fog	No	Poor	Excellent
Conversion Efficiency Performance limits for DC-to-RF & RF-to-DC conversion	OK	OK	Good
Required Aperture Size Transmit and receive antenna sizes	Small	Medium	Large
Safety Required due regard. Pointing. User perception.	OK	Good	Good
Economy of Scale Based on present state of the art to deliver 1000s of kW over 1000s of km	Poor	Poor	Good
	Small sites. Mobile platforms.		Large Power. Long Distance.

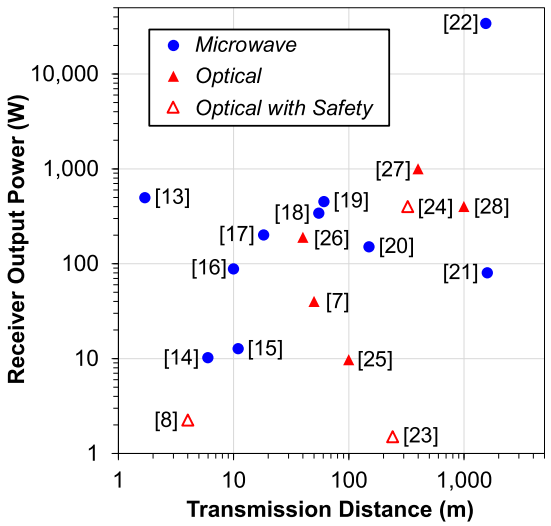

FIGURE 2. **Selected power microwave and optical power beaming demonstrations [7], [8], [13]–[28]. Optical demonstrations incorporating safety features are noted.**

cases abound in areas of growing interest. As illustrated in Fig. 1, power beaming can be used to deliver electrical power to any location where it is difficult to generate, e.g., unmanned systems such as unmanned aerial vehicles (UAVs) or balloons [5], remote installations such as forward operating bases (FOBs) [6], and industrial applications [7], [8]. In fact, power beaming is presently advocated as an "enabling technology" for 6G wireless communications [9].

There are three power beaming modalities: optical, mmWave, and microwave. Table 1 compares these. The chief advantage of optical power beaming is the small size requirement for the transmit and receive apertures. Although optical power beaming has recently made tremendous advances in performance [10], the technology is substantially dissimilar to microwave beaming and therefore outside the scope of this article. mmWave beams share many of the advantages of optical technology, but with the potential for enhanced safety, as indicated in Section VI of this paper. While optical and mmWave beams are best suited for beaming power to small sites or mobile platforms, microwave beams excel for high power, long distance applications. In the microwave range, atmospheric losses are extremely low [11], and both vacuum and solid state devices have higher f_{max}/f [12], resulting in higher performance limits for the achievable DC-to-RF and RF-to-DC conversion efficiencies. Importantly, where active microwave transmit arrays scale in power in proportion to their aperture area, scaling mmWave and optical transmitters to the MW regime and beyond raises significant challenges in terms of mechanical tolerances, power density, and cost at the current state of the art.

Fig. 2 provides an illustration of selected power beaming demonstrations to date [7], [8], [13]–[28]. W. Brown's 1975 Goldstone demonstration [22] remains the highest-power result to date, delivering 35 kW at 1.55 km. His other experiment of the same year [13] demonstrated the highest DC-to-DC power beaming efficiency result to date, delivering 495 W at 54% total system efficiency.

This paper is structured as follows: Section II provides an overview of the physics of power beaming, including beam diffraction and atmospheric propagation effects. Section III advocates a systematic approach for reporting the efficiency of power beaming demonstrations, which has been lacking to date. Section IV provides an historical overview of microwave and millimeter-wave power beaming demonstrations to the present date. Section V provides an historical overview of rectenna (i.e., rectifying antenna) arrays for the reception of beamed power, to the present state of the art. Section VI presents breaking developments in power beaming transmitter technologies. Section VII highlights regulatory issues, including spectrum management and safety. Section VIII concludes this paper.

II. THE PHYSICS OF POWER BEAMING

A. BEAM DIFFRACTION

Power beaming eliminates the infrastructure needed to transport power from the energy source to the energy consumer – exchanging wires, ships, and trains for the medium of free space. This dividend, however, comes with the requirement that the transmit and receive apertures be appropriately sized to minimize the effect of diffraction over the distance of the

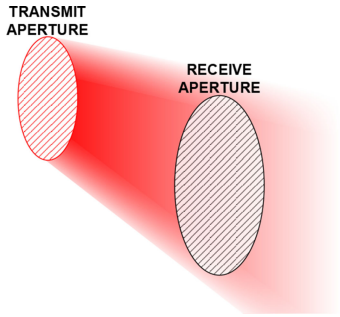

FIGURE 3. The beam collection efficiency is defined as the proportion of power radiated from the transmit aperture that impinges on the surface of the receive aperture. Any power projected beyond the edge of the receive aperture is lost.

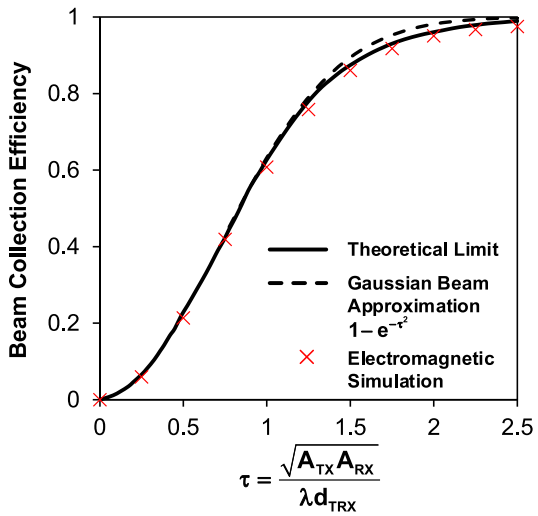

FIGURE 4. Beam collection efficiency as a function of transmit aperture area A_{TX}, receive aperture area A_{RX}, and distance between the transmit and receive apertures d_{TRX} for an optimal power beaming link operating at a wavelength λ.

power beaming link. The *beam collection efficiency* quantifies this tradeoff. Referring to Fig. 3, beam collection efficiency is defined as the proportion of the power radiated by the transmit aperture that impinges on the surface of the receive aperture.

Fig. 4 relates the beam collection efficiency over a given distance to the geometric mean of the transmit and receive aperture areas. Although developed for circular apertures, the result accurately approximates other aperture shapes, provided that the transmitter and receiver shapes are matched. Collection efficiencies approaching 100% are possible and have been achieved experimentally in the microwave [1] and mmWave regimes [29]. The theoretic limit [1], [30]–[32] assumes (1) that the apertures are aligned and (2) that the transmit amplitude and phase distributions are optimized for beaming power to the plane of the receive aperture. Note the common approximation used in Gaussian beam optics [33] tends to over-predict performance for efficiencies above 80%. Based on these curves, it is easy to show this important rule of thumb:

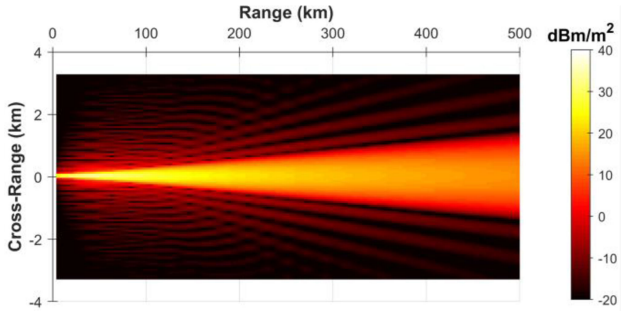

FIGURE 5. Diffraction from a 10-MW, 10-GHz, 30 m × 30 m transmit aperture whose amplitude and phase are optimized to deliver power to a 1 km × 1 km receive aperture located 400 km down range. Beam collection efficiency is 95%, which approaches the theoretic limit. This calculation uses the Huygens-Fresnel principal.

beam collection efficiency exceeding 15% is only possible if the link distance is less than the far-field distance of at least one of the two apertures.

where the far-field distance is defined according to [34] and the region inside this distance is referred to as the *Fresnel zone*.

Power beaming system design often involves a variety of practical constraints for which more detailed electromagnetic analysis and optimization are required [35], [36]. The Huygens-Fresnel principle [37] rigorously calculates complex field intensity vs. angle in both the Fresnel and far-field regions. Source code in [38] implements the technique numerically, adding the capability to (1) design the transmitter phase profile to create a spherically converging wave front at the plane of the receive aperture and (2) optimize the transmitter amplitude profile to a truncated Gaussian distribution. Optimized power beams calculated for a variety of geometries agree well with the theoretic limit, as shown in Fig. 4, validating this approach. This numeric method is also useful for visualizing power beaming links, as shown in Fig. 5, which illustrates the diffraction from a 10-MW, 10-GHz, 30 m × 30 m transmit aperture whose amplitude and phase are optimized to deliver power to a 1 km × 1 km receive aperture located 400 km down range. Beam collection efficiency is 95%, which approaches the theoretic limit.

Other computational approaches are possible. For example, the spatial frequencies of the transmit aperture can be calculated in the far-field [40] and propagated to a specific distance from the transmitter, provided that no approximations are made that are invalid [41] in the Fresnel zone. Detailed analytic approximations are also available [42], with some validation [43] against more general techniques.

Finally, terrestrial demonstrations of power beaming technologies often make use of existing transmitters optimized for far-field directivity rather than for beam collection efficiency at range. In these situations, the system tradeoffs can be non-intuitive to those accustomed to working in the far field regime only. Fig. 6 illustrates a case study based on a uniform transmit aperture, i.e., an aperture optimized for

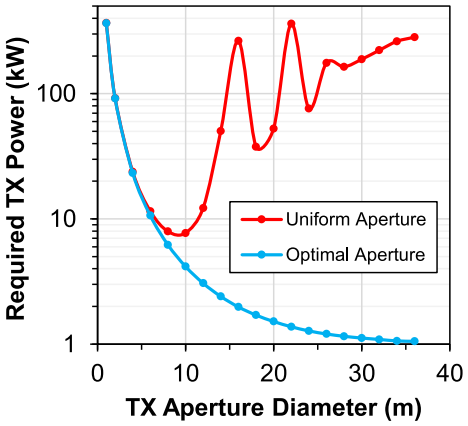

FIGURE 6. **Power needed at 10 GHz for a lossless circular aperture to project 1 kW onto a circular receive aperture of 2-m diameter located 1 km away. For the uniform case, using a transmit antenna optimized for far field directivity yields a non-intuitive result; increasing transmit antenna diameter beyond about 10 m greatly increases the transmit power requirement. The optimal case uses a phase and amplitude distribution designed to transfer power at a 1-km standoff.**

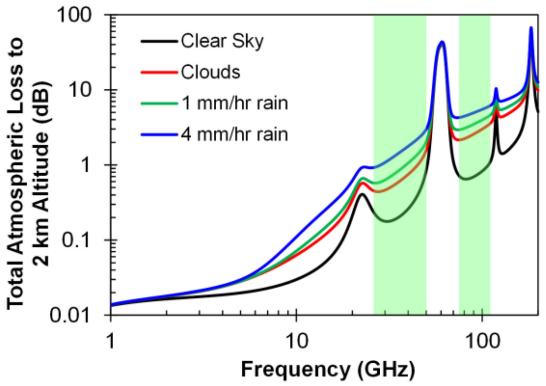

FIGURE 7. **Total atmospheric loss to beam power along a 45° line of sight from a sea-level transmitter to a receiver at a 2 km altitude. Surface temperature, pressure, and relative humidity are 288 K, 1013 mb, and 60%, respectively. Except for the clear sky case, clouds extend from 500 to 1500 m with a water vapor density of 0.33 g/m^3. The *Ka* and *W* mmWave bands are highlighted in green.**

far-field radiation efficiency. The transmit power needed at 10 GHz for a uniform, lossless circular antenna to project 1 kW onto a 2-m-diameter receive aperture located 1 km away is plotted vs. the transmit aperture's diameter, and compared with the performance of an aperture with amplitude and phase distributions optimized for power transfer over a 1 km link. For the uniform case, increasing transmit antenna size beyond a "sweet spot" of about 10 m in diameter actually increases the required transmit power. This result highlights how far-field gain and directivity concepts can lose validity in the Fresnel zone.

B. ATMOSPHERIC EFFECTS

Noise limited wireless systems, such as digital communications, typically operate with significant margin to atmospheric effects. I.e., the impact of weather to system function can be negligible if signal-to-noise-ratio remains above a minimum threshold at a given range.

For power beaming, however, there is no way to compensate for atmospheric loss; 1 dB of attenuation reduces efficiency by >20%, making atmospherics an issue of central importance. Fig. 7 presents a case study using validated atmospheric models [11], [44]–[49] to numerically calculate [50] the path integral of the loss along a 45° line of sight from a transmitter at sea level to a receiver at 2 km altitude. The plot shows total calculated loss vs. frequency from 0.1 to 200 GHz for several scenarios: clear sky, clouds, 1 mm/hour rain, and 4 mm/hour rain. Losses at 10 GHz and below are very low. The *Ka* and *W* bands highlighted in the figure represent the highest mmWave frequencies of practical interest for terrestrial power beaming, above which the atmospheric losses through clear air become excessive. Historically, although most power beaming demonstrations have taken place at the 2.45 and 5.8 GHz industrial-scientific-medical bands, *X* band has recently gained popularity as the highest microwave frequency range above which atmospheric losses begin to increase markedly [11].

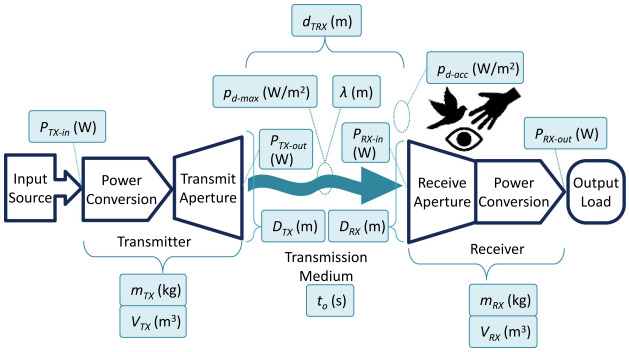

FIGURE 8. **The "15 Factors" for reporting power beaming system performance.**

III. BENCHMARKING THE PERFORMANCE OF POWER BEAMING LINKS

Reported results for power beaming systems and demonstrations are historically inconsistent, with few notable exceptions [51]. As power beaming becomes more prevalent as a means of moving energy, it is increasingly important to accurately and consistently characterize the performance details of competing systems. This paper advocates one paradigm for reporting measured results, to allow for fair and accurate benchmarking of performance between competing technologies.

A power beaming block diagram and selected measurable parameters are shown in Fig. 8. These 15 measurable parameters are defined and grouped in Table 2 by measurement type: length, power, power density, mass, volume, and time. Within each major grouping, measurable parameters proceed as appropriate from the input to the link to the output. These

TABLE 2 The 15 Factors, Defined

Parameter	Description
D_{TX} (m)	Maximum dimension of the transmitter aperture
λ (m)	Wavelength at the frequency of operation
d_{TRX} (m)	Distance between the transmit and receive apertures
D_{RX} (m)	Maximum dimension of the receiver aperture
$P_{TX\text{-}in}$ (W)	The power from all input sources to the transmitter
$P_{TX\text{-}out}$ (W)	Transmitter power output at frequency of operation
$P_{RX\text{-}in}$ (W)	The power incident on the receive aperture
$P_{RX\text{-}out}$ (W)	The arithmetic mean power at the output load
$p_{d\text{-}max}$ (W/m^2)	The maximum power density along the beam's path
$p_{d\text{-}acc}$ (W/m^2)	The maximum power density accessible to people, animals, aircraft, etc.
m_{TX} (kg)	The mass of the transmitter and transmit aperture
m_{RX} (kg)	The mass of the receiver and receive aperture
V_{TX} (m^3)	The volume of the transmitter and transmit aperture
V_{RX} (m^3)	The volume of the receiver and receive aperture
t_o (s)	The duration over which the demonstration occurred

parameters can be grouped differently depending on the principal interest of the demonstration performer or sponsor, or on the goals for the system. The 15 factors are equally applicable to microwave, mmWave, and optical power beaming links, where, in this context, "aperture" may be an antenna at microwave or mmWave frequencies, or a lens or reflector at optical wavelengths.

These parameters are by no means exhaustive, and are oriented with a single, simple, effectively stationary link in mind. For example, $p_{d\text{-}acc}$ is a safety metric indicating the maximum power density accessible to people, animals, aircraft, etc.; in a space-to-earth power beaming link, this parameter could be subdivided into multiple peak power densities corresponding to the different zones physically accessible to humans, birds, and aircraft based on the respective mobility constraints. Scenarios with multiple links, transmitters, or receivers may include other parameters of interest, as would those where transmitters or receivers are in motion—e.g, degree of sensitivity to misalignment, the ability to address multiple receivers simultaneously or in a time-shared manner, or any of a number of other novel features. These aspects should be described, quantitatively if possible. In addition, the categories of losses could be further subdivided depending on the system implementation and ability to quantify loss sources. For example, losses within the transmitter arising from thermal management systems, electrical power conversion, and optical or microwave component inefficiencies can enumerated separately.

To aid the clarity of depicting losses in a link or system, a Sankey diagram may be employed [54]. While perhaps ill-suited for illustrating precise uncertainties within the sources of inefficiency, Sankey diagrams are good for portraying major contributors to loss, as shown in Fig. 9 for notional power beaming demonstration. They also provide the confidence that the creator is mindful that the power beaming link is subject

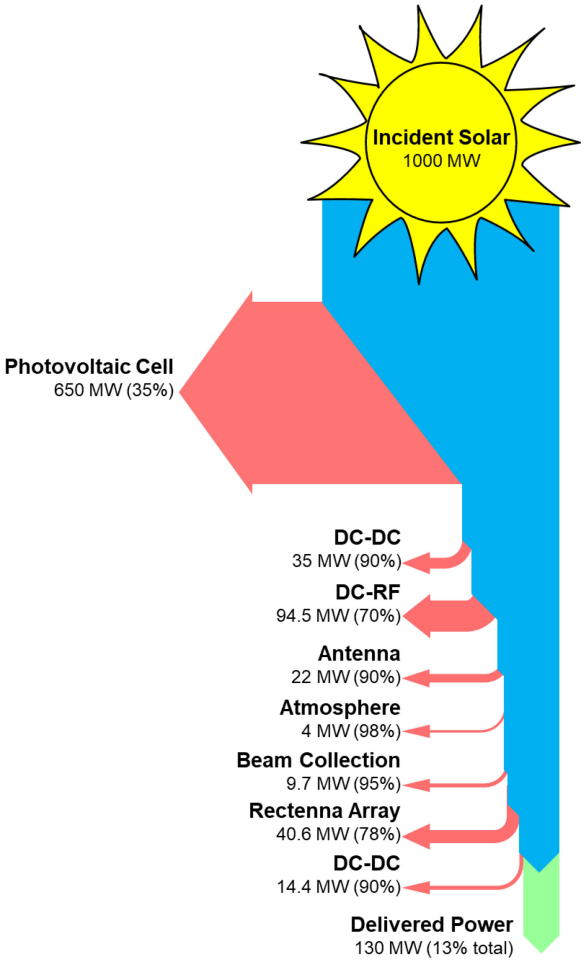

FIGURE 9. Sankey diagram for a notional SPS power beaming demonstration.

to the Law of Conservation of Energy since all significant sources or sinks of energy must be carefully accounted for.

For meaningful reporting, it is critical to be as clear as possible in defining what elements comprise the link and where the boundaries are. This can be accomplished by mapping the functional blocks in Fig. 8 to the hardware used in the demonstration. Transparency in the demarcation of where the system components are defined to begin and end is absolutely essential, as well as identifying the use and influence of any energy storage elements in the system. In describing the system, it may be helpful to acknowledge potentially legitimate alternative interpretations. For instance, is the boundary between the input source and transmitter defined by where a power supply plugs into an AC wall outlet, or by the output voltage supplied by the power supply? Is cooling equipment considered as part of the transmitter? In specific situations, different rationales could credibly justify accounting in one way or another. The key is to achieve clarity through the use of diagrams, photographs, and narratives.

Calculated parameters of potential interest are shown in Table 3. Many other system or component characteristics and

TABLE 3 Examples of Application-Specific Calculated Parameters

Parameter	Description
η_{BC}	Beam collection efficiency
L_P	Path loss between transmit and receive apertures
$E_{RX\text{-}out}$ (J)	Energy delivered to the receiver load
SP_{TX} (W/kg)	Transmitter mass-specific power
SP_{RX} (W/kg)	Receiver mass-specific power
η_{TX}	Combined efficiency of the transmitter's power conversion and aperture
η_{RX}	Combined efficiency of the receiver's power conversion and aperture
η_{Link}	End-to-end efficiency from the transmitter input to the receiver output

figures of merit are possible and may be significant for specific applications. This might include as area-specific mass (kg/m^2) [52], volume-specific power (W/m^3), or a host of others.

As with almost any engineered system, the result must typically balance the competing components of size, weight, power, and cost. For many applications, such economic concerns may be paramount or present additional driving significance. This has been explored by Dickinson [53], with the quantity $/MW-km introduced as a means of comparison. Depending on the circumstances, $/W, $/kWh, $/kg, or other cost factors or combinations of cost factors may be of principal concern. These could apply on either the transmitter or receiver side, or both. Even more broadly, system implementations will depend on an evaluation of technical, economic, legal, operational, and schedule factors.

IV. HISTORICAL OVERVIEW OF POWER BEAMING TRANSMIT TECHNOLOGIES AND DEMONSTRATIONS

Prior publications [55], [56] provide historical overviews of wireless power transmission. The following discussion focuses specifically on power beaming applications, extending the results to the present date, beginning with Tesla's experiments and ending with Naval Research Laboratory's recent orbital demonstration.

A. PRE-HISTORY (1900–1950)

Nikola Tesla originated the concept of large-scale power transfer via free space at the turn of the 20th century [57]. Tesla established plans to run alternating surges of current up and down a metallic mast in order to cause oscillations of electrical energy that would create a standing wave along the earth. Receiving antennas could then access power when placed within the standing wave maximum amplitude locations. Tesla first attempted to transmit power without wires at Colorado Springs, Colorado in 1899 using a huge "Tesla coil" over which rose a 61-m metallic mast with a 0.9 m diameter ball positioned at the top. The Tesla coil resonated 300 kW of low-frequency energy at 150 kHz. According to Tesla, when the radio frequency (RF) output of the Tesla coil was unleashed into the mast, 100 MV of RF potential was produced on the sphere. Although very large discharges of electrical energy were seen by people living in and around Colorado Springs, no significant power transfer was recorded at any distant point.

In the late 1940s, the advent of airborne radar, made possible by the introduction of both the klystron and magnetron, helped to bring about significant improvements in microwave sources, components, and antennas at frequencies through *X* band. During these years, the possibilities of microwave power beaming started to capture the imagination of American science fiction writers. In Isaac Asimov's short story "Reason", published in April 1941, two astronauts, residing at a space station, oversee the transmission of power to Earth via a microwave beam.

B. EARLY US CONTRIBUTIONS (1950–1980)

Progress in microwave power sources motivated the Raytheon Company to propose the Raytheon Airborne Microwave Platform (RAMP) concept in 1959 to the US Department of Defense as a solution to surveillance and communication problems. The proposed platform was a large helicopter positioned above the jet stream at 15,000 m where atmospheric winds are practically nonexistent. To fly at this altitude, the helicopter needed to be powered from earth by an Amplitron having an output of 400 kW of energy at 3 GHz with an efficiency over 80%. This high-powered Amplitron was developed in 1960 at Raytheon's Spencer Laboratory by W. Brown, who is largely regarded as the principal pioneer of the field of power beaming [58]. The only capability missing was the ability to convert microwave energy to DC power in order to drive motors attached to the rotor blades. The US Air Force awarded several contracts to study this rectification problem. One of the studies carried out by R. George at Purdue University showed that a semiconductor diode could be used as an effective rectifier [59]. At the same time, W. Brown at Raytheon carried out research on using a thermionic diode rectifier [60]. With the development of both high-powered sources and efficient rectifiers, power beaming for the first time became a feasible, and potentially useful, technology.

The US Air Force continued to partner with W. Brown and Raytheon during the early 1960s in the pursuit of emerging microwave power beaming possibilities. In 1963, the first modern system was constructed at Raytheon's Spencer Lab. This system, seen in Fig. 10(a), used a DC-fed magnetron and reflector to send microwave energy at 3 GHz to a horn antenna located 5.5 m away [61]. The horn was connected to a single close-spaced thermionic diode rectifier placed within the horn's waveguide section. DC rectified power of 100 W, corresponding to 15% DC-to-DC conversion efficiency, was seen across the diode's terminals. This demo resulted in a U.S. Air Force contract for remotely powering an airborne communications platform.

In 1963, W. Brown and R. George discovered that many solid-state diode rectifiers, operating in the 2 to 3 GHz range, could be combined within a waveguide and output reasonable amounts of DC power. To facilitate the test, George placed a

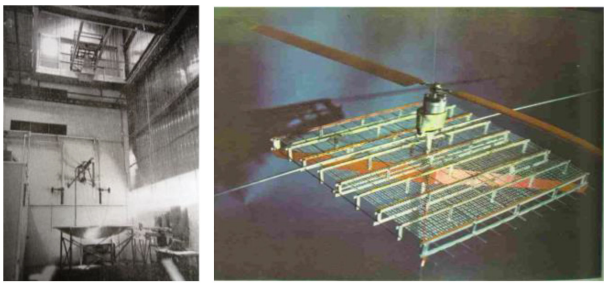

(a) (b)

FIGURE 10. Raytheon microwave power beaming experiments: (a) Raytheon Spencer Laboratory system. (b) microwave-powered helicopter.

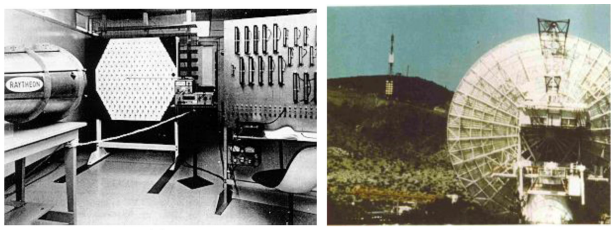

(a) (b)

FIGURE 11. Raytheon/JPL microwave power beaming experiments: (a) Raytheon setup that achieved 54.18% DC-to-DC system efficiency. (b) JPL Goldstone facility experiment.

dense array of diodes inside of a waveguide that was directly attached to a receiving horn [62]. The setup resulted in low efficiency numbers, so Brown and George moved the full-wave rectifiers outside of the waveguide over a reflecting plane. It was the first demonstration of a rectifying antenna (rectenna) array in which each half-wave dipole antenna element was assigned its own semiconductor diode. Brown, along with George, received a patent for the rectenna array [63], and their use of a ground plane has been copied in many of the most efficient rectenna arrays to date.

One of the most well-known power beaming demonstrations to the public occurred on October 28, 1964. The helicopter shown in Fig. 10(b) was flown for 10 hr at an altitude of 15.2 m [64] while powered by a microwave beam. The presentation was covered by Walter Cronkite's CBS news program, providing the world a glimpse of microwave power beaming's potential. Dipole antennas were used to collect the incoming microwave energy, and the DC energy that powered the propeller was obtained using 4,480 semiconductor diodes.

After the helicopter flight, the U.S. Air Force elected to discontinue their power beaming endeavors. Thus in 1967, W. Brown began to court von Braun and his staff at NASA's Marshall Space Flight Center (MSFC) on the possibilities of power beaming in space.

One such application of power beaming in space was the concept of space solar power (SSP) using solar power satellites (SPSs). This idea was first conceived by Dr. Peter Glaser of the Arthur D. Little Company in 1968 [65]. The SSP idea calls for a constellation of SPSs to be placed in geosynchronous orbit (36,800 km) in order to capture the sun's energy, convert it to microwave energy, and beam the power to Earth. Terrestrial "farms" of rectenna arrays would then collect the incoming energy and convert it to DC power [66].

In 1970, NASA MSFC awarded Raytheon a contract to improve the overall DC-to-DC efficiency of power beaming systems. The contract led to advances in solid-state rectifying diodes, improving the RF-to-DC conversion significantly. Another technological breakthrough enabling more efficient power beaming was the design of the dual-mode horn by P. Potter at the Jet Propulsion Laboratory (JPL) [67]. This modified horn launched a Gaussian beam with negligible sidelobes, improving the aperture transfer efficiency.

In 1971, W. Brown and P. Glaser, along with members of Northrop Grumman and the photovoltaic company Textron, conducted a six month study concluding that SSP had merit. A letter was then sent to the Director of NASA requesting funding [68], [69]. This led to NASA's Lewis Research Center (LeRC) awarded a small contract to Brown and his Raytheon colleagues for improving the overall efficiency of existing microwave power beaming systems, with the requirements necessary for a fielded SPS in mind. During the early 1970s, NASA began to shift more focus to SSP with JPL, under the guidance of R. Dickinson, who played a major role in the process. The culmination of efforts occurred in 1975 with the setup shown in Fig. 11(a) having an overall DC-to-DC conversion efficiency of 54%. This high efficiency was made possible by the fact that each rectenna was terminated into its own resistive load to compensate for the variability in power density on the rectenna array's surface, as dictated by the Guassian pattern distribution from the horn. The operating frequency was 2.446 GHz, and the rectenna array's output DC power level was 495 W. The end-to-end efficiency was certified by JPL's quality assurance organization and to this day stands as the highest power beaming end-to-end efficiency. The breakdown of the $54.18 \pm 0.94\%$ overall efficiency is $68.87 \pm 1.0\%$ for the DC-to-RF conversion and $78.67 \pm 1.1\%$ for the RF-to-DC conversion [69], [70].

In 1975, another important milestone was shown at the Venus Site of JPL's Goldstone Facility. In this demonstration shown in Fig. 11(b), microwave energy at 2.388 GHz was sent over a 1.54-km distance of the Mojave Desert to an awaiting 26.8-m^2 rectenna array. The rectenna array, designed by W. Brown at Raytheon, outputted 30 kW of DC power [71], [72]. Both the JPL certified, and Goldstone experiments gave NASA confidence regarding the viability of power beaming and its possible use in Glaser's SPS concept.

Between 1977 and 1980, NASA teamed up with the U.S. Department of Energy (DOE) to further evaluate SSP's potential in providing affordable energy to consumers on Earth. The resulting 670-page document determined that SSP was a feasible technology and should be pursued in the future [73]. One idea coming out of the study was the idea of retrodirectivity or the ability to keep the microwave beam on target. Unfortunately, the NASA sponsored program ended in 1980, causing the U.S. to lose its SSP leadership role.

(a) (b)

FIGURE 12. Microwave-powered SHARP aircraft designed as a small-scale model of a 21-km altitude airplane.

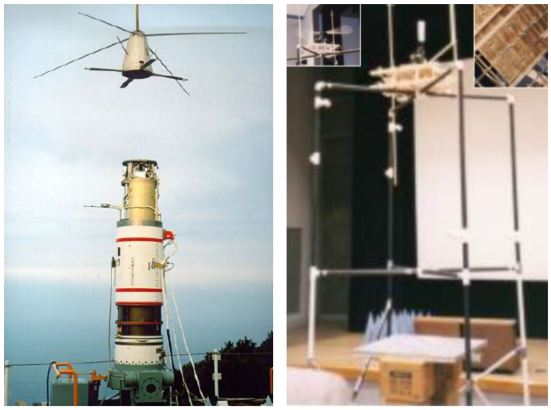

(a) (b)

FIGURE 13. Microwave power beaming experiments in the 1990s: (a) MINIX in Japan and (b) SABER in the US.

C. INTERNATIONAL INVOLVEMENT (1980–1995)

After 1980, microwave power beaming research and development shifted to Japan, with Canada also making contributions. In 1980, a program to develop a long endurance high altitude platform called the Stationary High-Altitude Relay Program (SHARP) was proposed in Canada [74]. The platform was to be the first unmanned, fuel-less, lightweight airplane powered remotely by microwaves, enabling it to stay airborne for 20 minutes. On September 17, 1987, the 1/8-scale prototype SHARP with a 4.5-m wingspan, seen in Fig. 12, flew on beamed microwave power for 20 minutes at an altitude of 150 m. A 2.45 GHz microwave beam was transmitted by a parabolic dish antenna, providing a power density at the airplane of 400 W/m^2. The dual-polarized rectenna array received enough microwave energy to generate 150 W of DC power to the electric motor in order to lift and fly the 4.1 kg airplane.

While demonstrations such as Goldstone and SHARP showed microwave power beaming's utility, automatic beam alignment between the RF transmitter and the rectenna array remained an issue. In 1987, researchers at Kyoto University, Kobe University, and Mitsubishi Electric Corporation developed the first retrodirective transmitter for microwave power beaming [75]. The 7-dipole 90-W transmitter could intentionally send energy in the direction of incoming pilot signals. It used a phase conjugation circuit to compare two asymmetric pilot frequencies in order to resolve the $2n\pi$ ambiguity in the phase comparison. Another retrodirective transmitter, developed later in 1996 by Kyoto University and Nissan Motor Co. Ltd., used pilot signals that were one-third the transmitting frequency. This simplifies the system design at the expense of a larger antenna for reception of the pilot signals. The Nissan system used a pilot signal of 815 MHz to keep 80 W of energy at 2.45 GHz on target.

Another example of driving a model airplane using microwave power was the MIcrowave Lifted Airplane eXperiment (MILAX) conducted by Japan in 1992. The experiment used an electronically scanned phased array to focus a 2.411 GHz microwave beam on an airplane. Two charge-coupled device (CCD) cameras recognized the airplane's outline revealing the location to a computer which scanned the array to the appropriate location. The transmitting array was located on a sports utility vehicle which was also in motion during the tests. MILAX received nationwide media coverage in Japan and endeared SSP favorably on the Japanese public [76].

Japan's status of being a large energy consumer with little natural energy resources has facilitated some well-funded programs exploring SSP as an alternative renewable energy source. Two of these programs have involved in-space experiments. The first of Japan's in-space experiments was the Microwave Ionosphere Nonlinear Interaction eXperiment (MINIX) conducted by Matsumoto and colleagues in 1983. MINIX focused on how the plasma wave dynamic spectrum changes when high-powered microwave energy is transmitted into ionospheric plasma [77], [78]. The second in-space experiment was the International Space Year – Microwave Energy Transmission in Space (ISY-METS) in 1993. In ISY-METS microwave energy was transferred from microstrip antenna arrays on one rocket to a second rocket carrying two different rectenna arrays, one of which had been designed in the US. ISY-METS represented the first example of power beaming in space [79].

In the 1990s, Brown's 1964 helicopter experiment inspired researchers at University of Alaska Fairbanks (UAF) to design and build a similar version pictured in Fig. 13(b). The program known as the Semi-Autonomous BEam Rider (SABER) used a JPL/Raytheon-designed slotted antenna array to transmit 2.45 GHz energy 3 m to the helicopter's rectenna array in order to drive a DC motor [80]. The motor caused the helicopter's propeller to rotate rapidly as the aircraft ascended two guideposts.

In 1994, Kyoto University, Kobe University, and Kansai Electric Corporation jointly developed the Ground-to-Ground Microwave Power Transmission (MPT) system [81] seen in Fig. 14(a). Here, 5 kW of magnetron-generated microwave energy at 2.45 GHz was fed to a 3-m parabolic antenna. The parabola then transmitted the power to a 3.2 m $\times$ 3.54 m

(a) (b)

FIGURE 14. Japanese power beaming experiments in the mid 1990s: (a) Ground-to-Ground MPT and (b) ETHER.

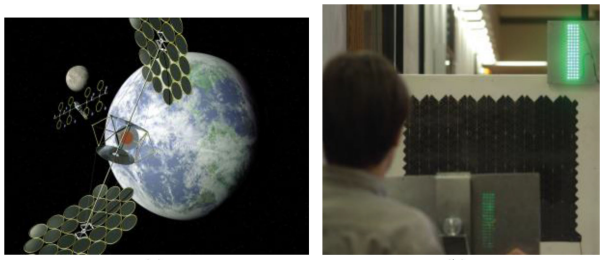

(a) (b)

FIGURE 15. SERT microwave power beaming systems: (a) "Clamshells" SPS, (b) World Space Congress CP demonstration, at reduced power to accommodate photography.

rectenna array (2,304 elements) located 42 m away. The beam efficiency was about 74%.

In 1995, N. Kaya of Kobe University constructed the airship seen in Fig. 14(b). This airship, constructed for the ETHER (Energy Transmission toward High-altitude long endurance airship ExpeRiment) program, received 10 kW of microwave power at 2.45 GHz [82]. The energy was transmitted from a parabolic antenna/dual magnetron system to the blimp's 3 m × 3 m (1200 element) rectenna array, allowing it to fly at a height of 50 m for four minutes.

D. ONGOING DEMONSTRATIONS (1995–2010)

NASA took notice of the Japanese successes and in 1995 undertook a series of studies reevaluating large-scale SSP systems [87] in terms of technical, economic, environmental, legal, social, and regulatory considerations. In 1999, NASA MSFC started the SSP Scientific Exploratory Research and Technology (SERT) Program, resulting in successful demonstrations on a variety of system level SPS components, as well as new SPS design concepts such as the integrated symmetrical concentrator (ISC) SPS, affectionately known as the "clamshells" model. An artistic rendering of this SPS concept, presented in Fig. 15(a), shows two opposing ultralightweight arrays of solar-sail concentrator mirrors, contained within space frame structures, to illuminate photovoltaic arrays positioned on a centrally-located transmitting body. The mirrors were to always face the sun with very little, if any, shadowing. The transmitting body would then generate the microwave energy and beam it to Earth.

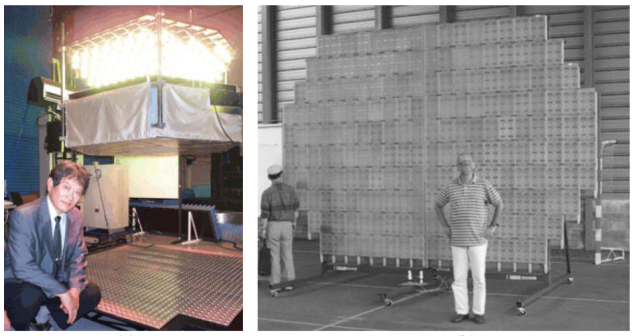

(a) (b)

FIGURE 16. Microwave power beaming programs developed in the 1990s: (a) SPRITZ and (b) the Reunion Island rectenna.

In 2002, a SERT-sponsored public demonstration at the World Space Congress in Houston, TX illuminated a 1-m rectenna array with a circularly polarized (CP) beam at 5.8 GHz, demonstrating 82% RF-to-DC conversion efficiency [88]. The transmitter [89] featured retrodirective control so that the beam could track the rectenna array as it manuevered along the exhibition floor. This joint demonstration of Texas A&M University and NASA Johnson Space Center was witnessed by media, international officials, and more than 10,000 members of the public.

Meanwhile, the SPRITZ program at Kyoto University culminated in 2000 with a fully integrated solar power radio transmitter. This system seen in Fig. 16(a) was exhibited at the 2002 World Space Congress in Houston, TX. The system used 133 75-W halogen lamps to provide the photons for illuminating the solar cells. The solar cells output 166 W at 15% efficiency. The 5.8-GHz microwave transmitter had 3-bit phase control and 25-W output power. The rectenna array had 1,848 individual rectennas providing the DC power for illuminating LEDs [83].

In 2001 on Reunion Island in the Indian Ocean, researchers from the University of La Reunion unveiled an industrial prototype rectenna pictured in Fig. 16(b) as a first step toward the goal of one day supplying the isolated village of Grand-Bassin on Reunion Island with remotely derived energy [84], [85].

During the 1995–2000 period, South Korea also initiated microwave power beaming projects. Dr. K.H. Kim of Korea Electrotechnology Research Institute (KERI) demonstrated the power beaming system shown in Fig. 17. The transmitter used a magnetron driving a parabolic dish antenna to beam power to a rectenna array 50 m away. The rectenna used a 2016-element array of dual-polarized microstrip patch antennas with a frequency-selective surface in front. The transmitter power and receiver DC output were 2.3 kW and 1.02 kW, respectively, for a total power beaming efficiency of 44% [86].

In 2001, the Japanese Aerospace Exploration Agency (JAXA) announced an SPS design that could beam 1 GW of RF power at 5.8 GHz [90]. In 2000 and 2001, Kyoto University unveiled two microwave power beaming systems known as SPORTS-2.45 and SPORTS-5.8. Semiconductor

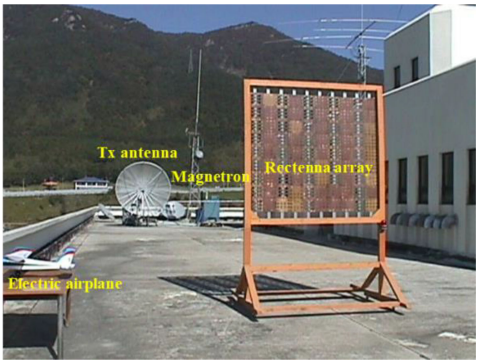

FIGURE 17. Microwave power beaming system setup in KERI in Korea

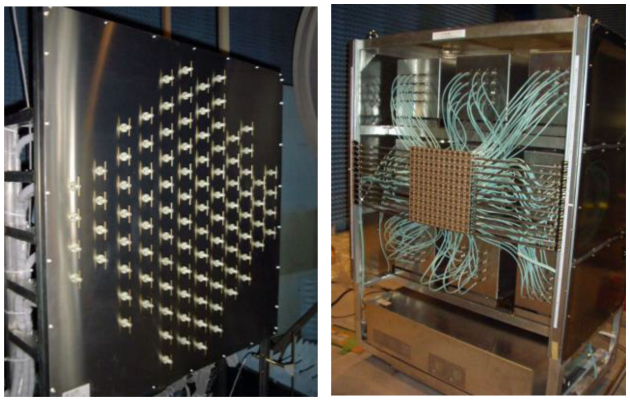

(a) (b)

FIGURE 18. SPORTS PCM-based transmitters: (a) 2.45 GHz and (b) 5.8 GHz.

technology had been unable to provide high-efficiency beamforming at kW power levels. To overcome this, the Space Power Radio Transmission System (SPORTS) demonstrations used arrays of phased-controlled magnetrons (PCMs) injection locked via phase lock loop (PLL) feedback [91], an idea originally from Brown, to circumvent the need for high-power, high-efficiency microwave solid-state power amplifiers. The PCMs were purposely limited to a couple hundred watts to eliminate the need for power division between the PCMs and the radiating elements. Certain SPORTS array configurations allowed for each array element to have its own PCM which decreased system losses and the amount of heat generated. SPORTS-2.45 was equipped with an outdoor solar cell panel supplying 8.4-kW DC to 12 PCMs that combined to output 4 kW of 2.45-GHz power. The RF power was then inputted into a 12-element horn or into the 12 × 8 dipole retrodirective (400 MHz pilot) electronically steered phased array (2 kW at 2.45 GHz) seen in Fig. 18(a). Lastly, this RF power was transmitted to a planar 2,692 element Yagi-Uda rectenna array for conversion back to DC. SPORTS-5.8 used 144 microstrip antennas and 144 4-bit phase shifters to beam 7 W of power at 5.8 GHz to a rectenna array. Unlike SPORTS-2.45, SPORTS-5.8 used a collection of rectenna panels that could be morphed into different geometries, namely planar or quasi globular [92].

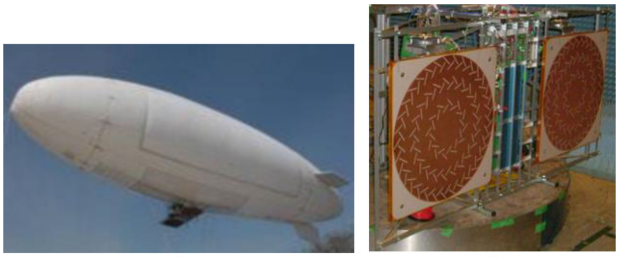

(a) (b)

FIGURE 19. Airship-to-ground experiment: (a) blimp, (b) radial slot array.

In 2008, the University of Kobe collaborated with Texas A&M University on a widely publicized demonstration covered live on US television. The experiment transmitted power from Maui to the big island of Hawaii, over a 148 km distance but with a beam collection efficiency of <0.001% [93], [94].

A year later in 2009, Kyoto University fielded another experiment using the PCM technology in which power was beamed from an airship to the ground, indicative of a small-scale power beaming system. Two 110-W PCMs generated 2.46-GHz microwave power which was then fed individually to two radial slot antennas located on the underside of a blimp as seen in Fig. 19(a). Each of the 72-cm diameter slot antennas pictured in Fig. 19(b) had a gain and aperture efficiency of 22.7 dB and 54.6%, respectively. The system employed retrodirective tracking at 5.8 GHz, making the pilot frequency higher than the microwave power beaming frequency [95]. This differed from previous designs where the retrodirective frequency was lower, and thus the pilot antenna size could be made smaller.

E. INTENSIFIED ACTIVITY (2010–2020)

The last decade has witnessed significant intensification of power beaming activities worldwide, as political support for the technology has materialized in Japan, South Korea, China, and the US.

1) JAPAN

In 2009, the Japanese Ministry of Economy, Trade and Industry (METI) initiated an SPS research committee chaired by N. Shinohara of Kyoto University. By the end of the following decade, the committee would succeed in three large field experiments of microwave power beaming.

On February 24, 2015, Mitsubishi Heavy Industries, Ltd. (MHI) announced that they had set a microwave power beaming record in Japan by transmitting 10 kW of 2.45-GHz RF power over a 500-m distance [97]. The test was conducted on a pier at the Kobe Shipyard and Machinery Works in Hyogo Prefecture. The transmitter used phase controlled magnetrons based on Kyoto University design [98]. The magnetron and rectenna arrays used in the test are shown in Fig. 20. Both are 8 m × 8 m. The power received was used to light up the MHI logo as seen in Fig. 20(b).

(a) (b)

FIGURE 20. MHI 2015 Experiment: (a) PCM transmit array and (b) rectenna array.

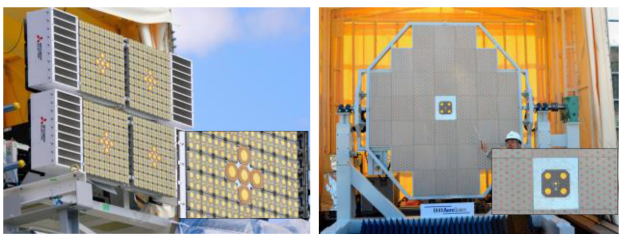

(a) (b)

FIGURE 21. JAXA 2015 Experiment: (a) phased array transmitter and (b) rectenna array.

On March 8, 2015, the METI SPS team successfully carried out a horizontal ground microwave power beaming experiment at the Mitsubishi Electric Facility in Hyogo Prefecture. The phased array pictured in Fig. 21(a) took six years to complete and was equipped with state-of-the-art GaN amplifiers [99]. Its four phased array panels combined to transmit 1.8 kW of 5.8-GHz microwave energy over a 55-m distance to the rectenna array shown in Fig. 21(b). The received rectified power was about 335-W DC. The system implemented retro-directivity at 2.45 GHz for each of the four individual phased arrays [114], [115]. The pilot arrays are shown central to each transmit array as well as the rectenna array. Prior to the outdoor experiment, exhaustive laboratory testing was done in which the four phased array panels were slightly misaligned orthogonally from their ideal planar configuration. The retrodirective subsystem was able to maintain beam pointing at the rectenna. This analysis is directly applicable to an SPS which may experience subtle moment-generated deformations in space. The phased array was composed of four 2.5 cm × 60 cm × 60 cm panels each weighing 16.1 kg. Each panel included 76 GaN class-F amplifiers, whose average amplifier efficiency was 60.3%, and total efficiency (DC–RF) was 35.1%. Each amplifier connected to a 4-antenna subarray. A 2.6 m × 2.3 m rectenna array developed for the field experiment used 36 rectenna modules with the Schottky diode rectifiers. RF–DC conversion efficiency was 59% (diodes distributed from 59% to 62%). The total receive efficiency, including the 96% efficiency of the power distribution unit, was 42%. The R&D project was conducted by J-Space System. The phased array and the rectenna array were developed by Mitsubishi Electric Corp. and IHI Aerospace Co., Ltd., respectively. Japan Aerospace Exploration Agency played a role of beam-steering experiment in the METI project.

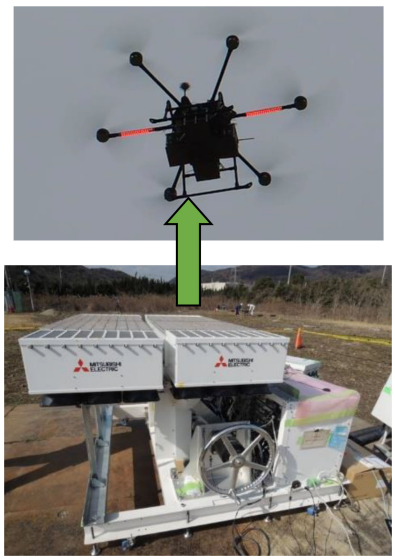

FIGURE 22. Japanese field experiment beaming power to a flying drone in 2019.

In May 2019, the third METI experiment successfully beamed power to a flying drone [100], as shown in Fig. 22. This experiment reused the phased array showing in Fig. 21 and developed a new small and lightweight rectenna whose size was 200 mm × 186 mm with 17 circular microstrip antennas [101]. The microwave power density was 4 kW/m^2 at the drone at a distance of 10 m. The DC output power was approximately 60 W. The drone could also receive approximately 42 W at 30 m. Although this received power was insufficient to fly the drone without the battery, the beamed power was able to extend the battery life and therefore the drone flight time.

On the basis of these successes, the METI SPS committee began developing a sandwich structure with microwave phased array and solar cells in 2019, with expected completion in 2024.

In other work, Tsukuba University developed a 303-GHz rectenna in 2018 [102] using the MACOM MA4E1317 GaAs Schottky diode shown in Fig. 23. The measured efficiency was 2.17% for 17.1 mW output DC power. A custom GaN Schottky diode is in development to increase the efficiency in sub-THz rectennas [103]. Power beaming in this frequency range could be suitable for future exoatmospheric applications where propagation losses do not play a significant factor.

2) SOUTH KOREA

In 2019, Korean and US researchers beamed power at 10 GHz to an airship [104], allowing it to maneuver at 7 mph

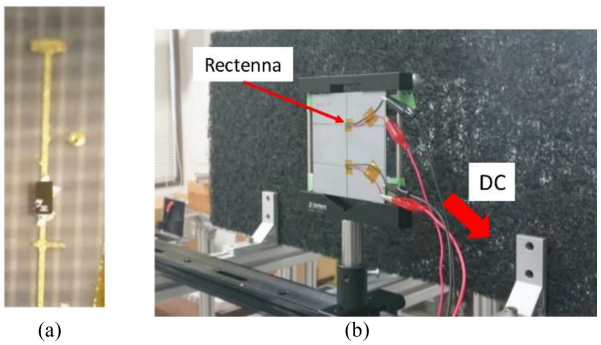

(a) (b)

FIGURE 23. (a) 303 GHz rectenna with GaAs Schottky diode, notch filter, and antenna. (b) Experiment measuring the efficiency of rectennas using a 303-GHz gyrotron.

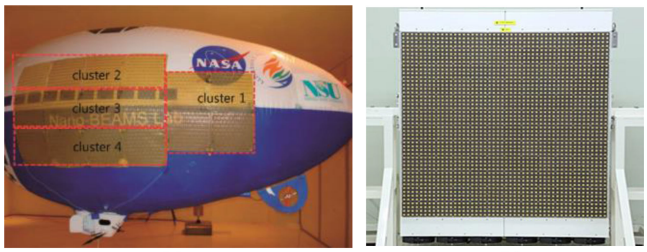

(a) (b)

FIGURE 24. (a) Joint US-Korean microwave powered airship; (b) RF Core phased array transmitter.

(a) (b)

FIGURE 25. Chinese SPS prototype hardware in indoor demonstrations (a) Chonquing phase-controlled source and rectenna array and (b) Xi'an focused CP experiment.

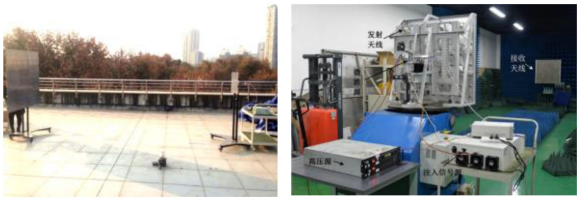

(a) (b)

FIGURE 26. Chengdu microwave power beaming experiments at (a) 2.45 and (b) 5.8 GHz.

within NASA Langley Research Center's High Intensity-Radiated Fields (HIRF) chamber. The airship utilized 16 etched flexible-circuit-membrane rectenna array sheets, each containing 90 half-wave dipole elements, on either side of the craft, for 32 in total. The craft is shown in Fig. 24(a). Also, recently, a Korean company—RF Core—has developed X-band microwave power transmitters [105]. The design is a 2304-element GaN MMIC-based phased array with 1.5 kW transmit power, shown in Fig. 24(b).

3) CHINA

As with other areas of technical endeavor, China is increasing its activity in microwave power beaming. In fact, Vice-President Z. Pang of the China Academy of Space Technology (CAST) made a statement to the media in 2019 that "China is expected to become the first country to build a space solar power station with practical value" [106]. To this end, the Chinese SPS Promotion Committee was founded on January 17, 2018. The committee is a voluntary non-government organization composed of professors and engineers from research institutions interested in SPS. As announced on December 6, 2018, a SPS experiment base is being established in Chongqing. The main purpose will be to demonstrate power beaming technology and a complete SPS system based on an airship. The experiment base will cover an area of 130,000 m^2, at a total investment of $30 million. Future plans include major science and technology infrastructure. Related to this effort, in 2020, Chongqing University unveiled the phase-controlled source, transmit antenna, and power sub-system shown in Fig. 25(a). Before the end of the year, the university intends to demonstrate a 5.8-GHz, 640-W power beaming experiment at a distance of 60-100 m using a 64-channel phase-adjustable microwave source [107].

In 2018, researchers in Xi'an detailed the focused CP microwave power beaming system seen in Fig. 25(b). The CP rectenna array achieved 66.5% RF-to-DC conversion efficiency [108]. In December of the same year, another SPS project named ZhuRi (Chase the Sun) was announced to demonstrate a complete SPS system on the ground based on OMEGA SPS—one of the Chinese SPS concepts [109]. The project will be led by Prof. D. Baoyan of Xidian University.

In parallel with these SPS-focused efforts, there are significant microwave power beaming research programs operating in other regions of China, including Chengdu and Wuhan. In 2014, Prof. C. Liu's group of Sichuan University, Chengdu, utilized a rectenna array whose maximum output power was 7.1 W at 2.45 GHz, shown in Fig. 26(a). They performed a 4.5-m microwave power beaming experiment whose overall efficiency reached 14.2% [110]. In 2016, they proposed a "subarray decomposition" rectenna technology. In experimental results at 5.8 GHz, they verified that the technique can improve the efficiency more than 10% [111]. In 2020, Prof. X. Chen's research group, also at Sichuan University, designed and implemented a 5.8-GHz microwave power beaming system operating over a 10-m distance with overall efficiency of 18.5%, as shown in Fig. 26(b) [112].

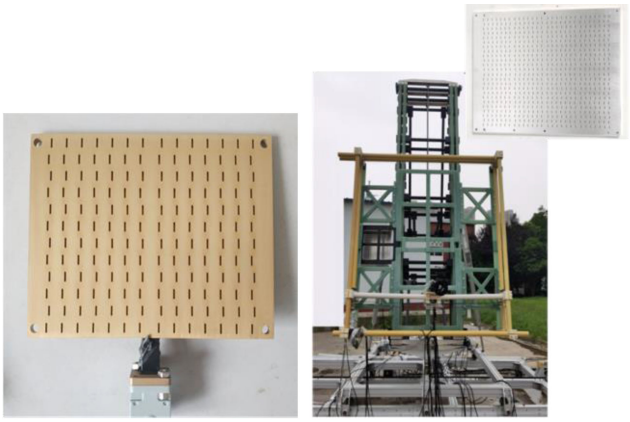

(a) (b)

FIGURE 27. (a) 35 GHz spatiotemporal transmitting antenna; (b) receiving system and 35 GHz spatiotemporal receiving antenna in Wuhan in 2020.

In Wuhan, Dr. L. Xiao of the China Ship Development and Design Center has disclosed a far-field "diffraction-free" mmWave power beaming design that eliminates the divergence of an electromagnetic wave. This concept uses a spatiotemporal beam (i.e., a beam in which each spatial frequency is assigned to a single wavelength) to beam power to the far-field without diffraction. In a 2020 experimental demonstration, approximately 1-kW of power was beamed at 35 GHz over a 300-m distance. The experiment used a spatiotemporal antenna, a custom mmWave tube transmitter, and a custom GaN diode for the rectenna. The transmit and receive apertures are shown in Fig. 27. A total efficiency of 9.89% was achieved from 220 VAC at the transmitter input to 36 VDC at the receiver output. This work was supported under the State Grid Corporation of China project "Research on Ten-Meter-Level Microwave Radio Wireless Power Transmission Technology." Before the mmWave experiment, the group had already succeeded in a 10-GHz microwave power beaming experiment in 2019 at a distance of 100 m; the efficiency from 220 VAC to 24 VDC was approximately 19.5%. This 10-GHz experiment also featured a custom microwave tube design and GaN diode rectenna [113].

4) UNITED STATES

In 2016, the D3 Space Solar Proposal was announced with the expressed goal of the United States becoming a leader in the development of SSP. The initial proposal was integrated into the United States' "3 Ds of foreign policy" framework, namely diplomacy, defense, and development. The proposal recognized that many other nations have active SSP programs while the U.S. did not. The signatories have both technical and political backgrounds, representing such entities as the U.S. Department of State, U.S. Department of Defense, Defense Advanced Research Projects Agency (DARPA), USAID, US Naval Research Laboratory (NRL), US Air Force, and Northrop Grumman [116].

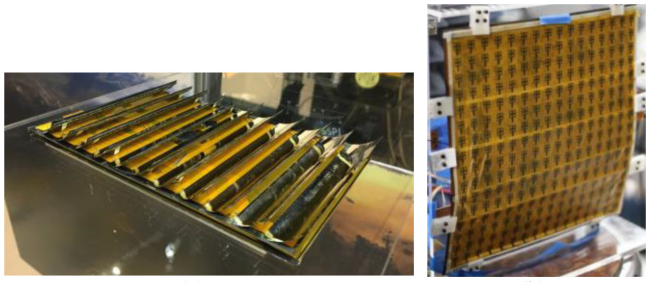

(a) (b)

FIGURE 28. (a) Caltech / Northrup Grumman photovoltaic phased array [122]. (b) Caltech flexible RFIC based phased array [120].

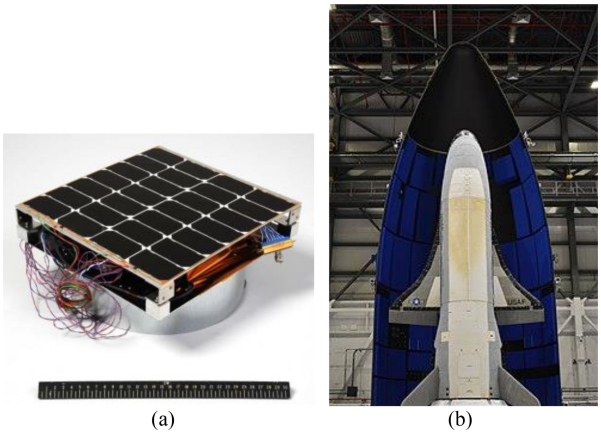

(a) (b)

FIGURE 29. NRL 2020 SSP experiment: (a) PRAM, (b) the X-37B orbital test vehicle.

In 2018, a collaboration between Caltech and Northrop Grumman Corporation developed an ultralight, high efficiency photovoltaic phased-array system. The design, shown in Fig. 28, distributed power dynamically and featured ultralight deployable space structures [117], [118]. Late in 2019, Northrop Grumman announced that it is working with the US Air Force Research Laboratory (AFRL) on the Space Solar Power Incremental Demonstrations and Research (SSPIDR) project to develop a SSP system [119]. In 2020, the Caltech team announced several innovations that advance SPS power beaming, including flexible RFIC based phased arrays with dynamic calibration [120], [121] and timing devices for large-scale phased array synchronization [122].

On May 17, 2020, the US Naval Research Laboratory (NRL) launched its Photovoltaic Radio-frequency Antenna Module Flight Experiment (PRAM-FX) aboard an Air Force X-37B orbital test vehicle. PRAM-FX, shown in Fig. 29, is a 12-inch square tile that collects solar energy and converts it to RF microwave power [124].

V. HISTORICAL OVERVIEW OF RECTENNA ARRAYS FOR THE RECEPTION OF MICROWAVE BEAMS

Over the last 50 years, there have been hundreds of publications on individual rectenna elements for the reception of microwave power. Efficiencies for some of the best performing

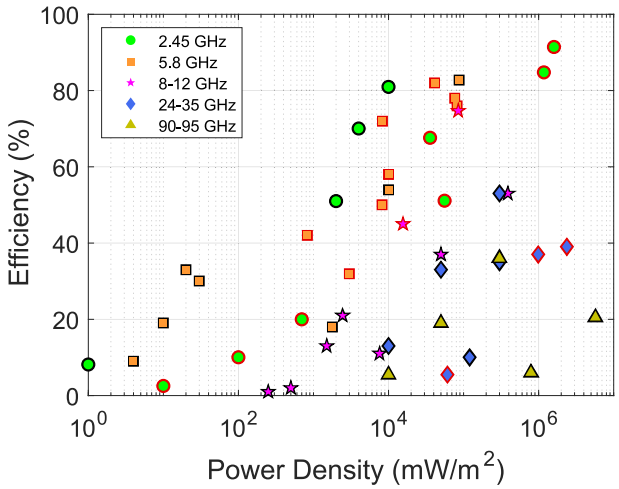

FIGURE 30. Rectifier efficiencies versus power density (P_D) for different frequencies. Markers with black outlines have efficiency defined as P_{DC}/P_{REC}, where P_{REC} is the RF power received by the antenna. Red outlines define efficiency as $P_{DC}/(A*P_D)$, where A is the rectenna area. Markers with no outline are stand-alone rectifiers.

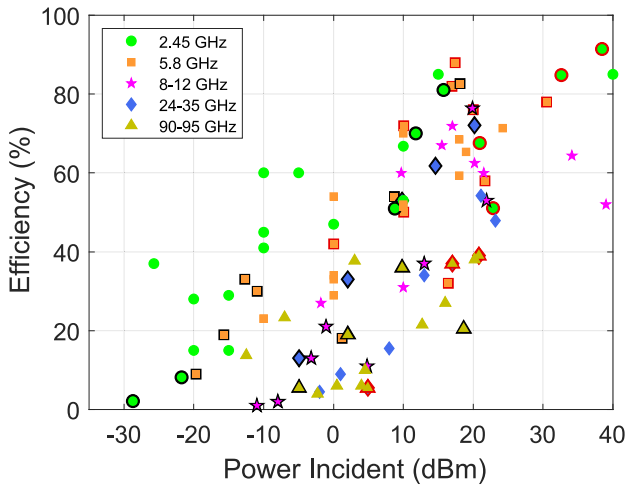

FIGURE 31. Rectifier efficiencies versus incident power for different frequencies. Markers with black outlines have efficiency defined as P_{DC}/P_{REC}, where P_{REC} is the RF power received by the antenna. Red outlines define efficiency as $P_{DC}/(A*P_D)$, where A is the rectenna area. Markers with no outline are stand-alone rectifiers.

rectennas to date are plotted in Fig. 30 and Fig. 31. Fig. 30 presents RF-to-DC rectifier efficiency in terms of incoming power density, whereas Fig. 31 plots efficiency vs. incident power. The lower number of data points in Fig. 30 results from the lack of information for some reported results. Data show are at 2.45 GHz [125]–[137], 5.8 GHz [134]–[148], 8–12 GHz [149]–[155], 24–35 GHz [155]–[163], and 90–95 GHz [163]–[170]. The best published efficiencies are just over 80%, with lower frequency rectennas typically having superior efficiency to those designed at higher frequencies. Higher efficiencies are also obtained when the input power to the diode is higher. The highest efficiency reported is W. Brown's 91.4% efficient rectenna operating at 2.45-GHz with 7-W input power [135];

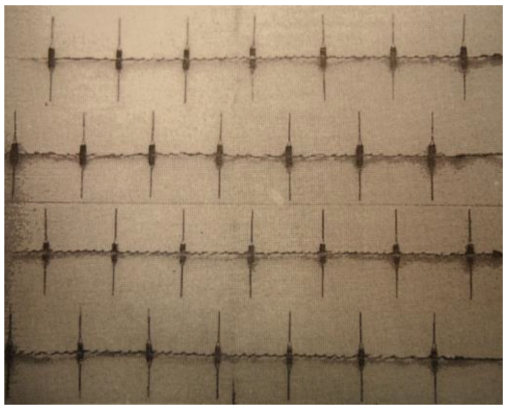

FIGURE 32. The first rectenna.

the design used a custom diode technology and primarily air/metal construction.

For concision, and for maximum relevance to power beaming applications, this section focuses on novel rectenna arrays where numerous rectenna elements are combined. Arrays developed by corporate, government, and/or academic partnerships from a variety of countries are included. Effort is given to present rectenna arrays that have not been previously covered while striving for geographic diversity.

A. THE FIRST RECTENNA DESIGNS

The first rectenna array was conceived at the Raytheon Company in 1963 by W. Brown. The rectenna array, seen in Fig. 32 was subsequently built, and tested by R. George of Purdue [171], [172]. It was composed of 28 half-wave dipoles with lead lengths sized to resonate at 2.45 GHz. Each dipole was terminated into a bridge rectifier made from four 1N82G point contacts. The rectenna array was suspended approximately $\lambda_0/4$ at 2.45 GHz in front of a metallic reflecting plane for a 3-dB radiation enhancement in the desired boresight direction. The DC rectified power generated from each row passed along twisted pair wires to DC bussing where row contributions combined. The array achieved about 40% rectification efficiency with an output of 7 W DC.

Given the difficulty of positioning the diodes accurately in terms of spacing and precise polarization alignment, Brown at Raytheon, working now with R. Dickinson of NASA's Jet Propulsion Laboratory (JPL), would eventually opt for the much more robust and aligned 3-D volumetric design illustrated in Fig. 33(a). In this approach the rectenna element, consisting of a 1) half-wave dipole, 2) low pass input filter, 3) Schottky barrier diode, and 4) RF bypass capacitor was inserted through a reflecting plane surface. On one side of the plane, the dipole received power, and, on the other side, bussing distributed DC power to a collective resistive load. The 3-D rectenna is shown in Fig. 33(b) along with its equivalent circuit [173].

The rectenna type of Fig. 33 supported two well-known Raytheon/JPL rectenna array demonstrations. In the first test, 199 rectenna elements within the array of Fig. 34(a) were

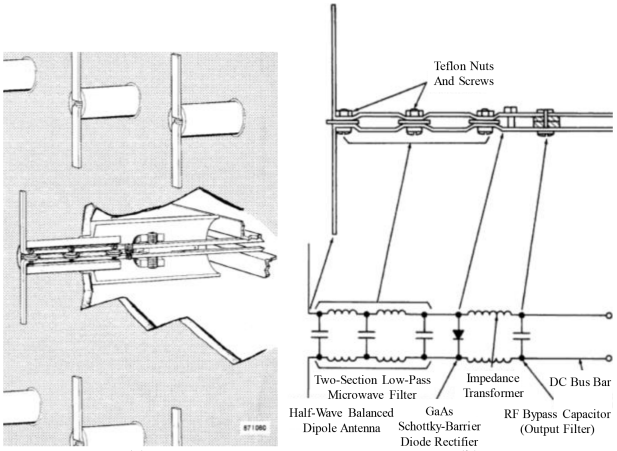

FIGURE 33. Raytheon/JPL rectenna design: (a) array implementation and (b) rectenna illustration with equivalent circuit.

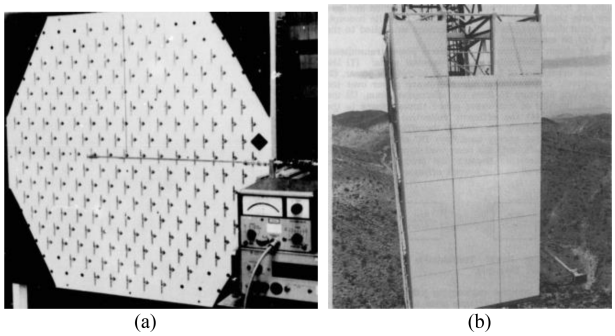

FIGURE 34. Raytheon/JPL rectenna arrays: (a) 54.18% DC-to-DC system efficiency and (b) Goldstone's Venus Site experiment.

oriented into a hexagonal format with each having its own resistive loading. This variability in resistive loadings allowed the rectennas to account for different received powers generated from the concentric rings of power densities incident upon the rectenna array's surface. In addition, a low pass filter and RF bypass capacitor trapped harmonic energy for further mixing at the diode to accumulate even more DC. The resulting RF-to-DC conversion efficiency was 78.67% $\pm$ 1.1% [174]. A prior experiment with the same rectenna array, in which the elements were terminated into only one communal resistive load, resulted in the DC-to-DC conversion efficiency being 4% less and so the "individual loadings" approach was adopted.

The second test was the famous Goldstone experiment with the Reception-Conversion (RXCV) array shown in Fig. 34(b), the largest rectenna array to date. The 24-m^2 (3.4 m $\times$ 7.2 m) RXCV array consisted of 17 subarrays with each subarray having 270 rectenna elements arranged in an equilateral triangular grid. A large reflecting antenna, located 1.54 km away, illuminated the rectenna array's surface with peak RF intensities of up to 170 mW/cm^2 at 2.388 GHz, yielding 30.4 kW of rectified DC output power. The highest RF-to-DC conversion efficiency measured was greater than 80% [173].

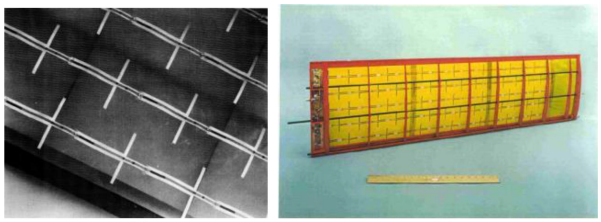

FIGURE 35. Linearly polarized 2.45 GHz half-wave dipole rectenna arrays: (a) W.C. Brown's "thin-film" and (b) SHARP's wing.

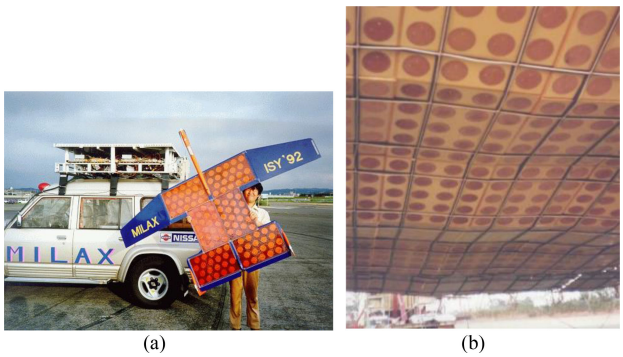

FIGURE 36. Japanese dual-polarized rectenna arrays: (a) MILAX and (b) ETHER.

While Goldstone showed that a large rectenna array could remotely output large amounts of DC power with good efficiency, the form factor, weight and fabrication difficulties associated with the array(s) were not desirable. In 1980, Brown introduced a "thin-film" rectenna made using photolithographic techniques. One of Brown's half-wave dipole thin-film arrays is seen in Fig. 35(a). This array fitted the harmonic-rejection filtering, diodes, and RF bypass capacitors along coplanar striplines. This kept everything, including the DC collection, in one plane. The rectenna array was suspended $\lambda_0/4$ above a ground plane in order to enhance the antenna element gain. Brown showed that individual rectennas of this type can achieve RF-to-DC conversion efficiencies at 2.45 GHz over 80% [175].

B. AIRBORNE RECTENNAS

On September 17, 1987, Canadian researchers carried out the Stationary High-Altitude Relay Program (SHARP) demo [176]. The rectenna array was distributed over the underside of the plane, including the wings, as seen in Fig. 35(b), and under a large rectenna disk towards the back of the plane. Linearly polarized half-wave dipoles were used, operating very similar to Brown's "thin film" array developed several years earlier.

Japanese researchers at Kobe University and Kyoto University, in the 1980s and 1990s, introduced orthogonally fed dual-polarized circular patch radiators into etched rectenna arrays, most notably MILAX in Fig. 36(a) and ETHER in Fig. 36(b). The circular patches were advantageous since their harmonic

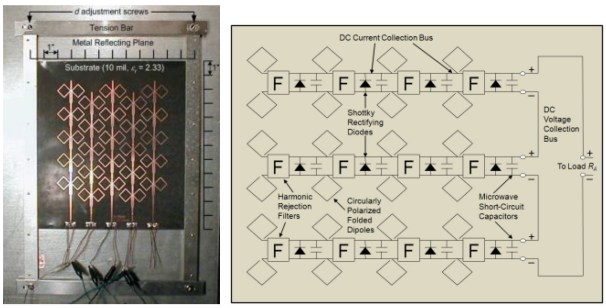

FIGURE 37. **(a) Texas A&M CP rectenna array. (b) Diagram showing components and DC collection for similar CP rectenna array.**

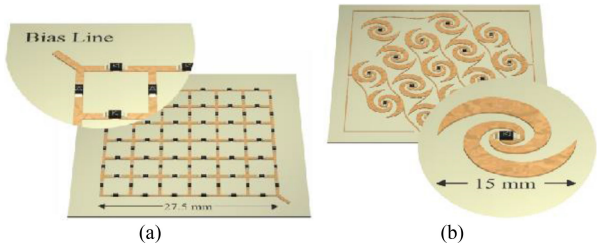

FIGURE 38. **University of CO rectenna arrays: (a) grid and (b) spiral. Black rectangles are Schottky diodes.**

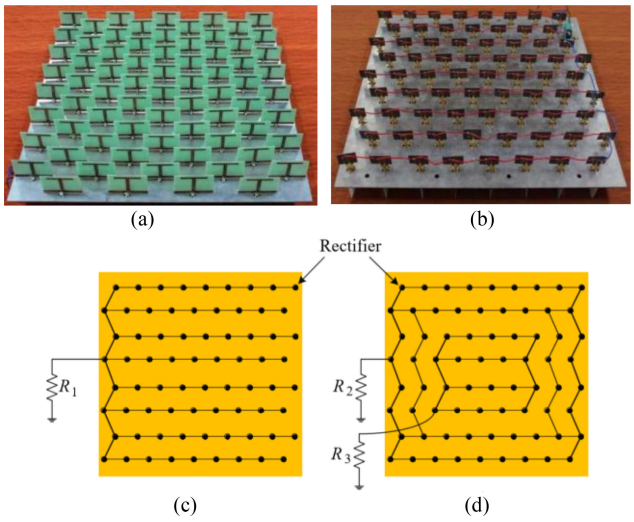

FIGURE 39. **Connectorized dipole rectenna array: (a) dipoles, (b) rectifier circuits, (c) loading for plane wave, and (d) loading for "short distance". R_1 is 10 Ω; R_2 and R_3 are 15 Ω and 25 Ω, respectively.**

frequencies, determined from Bessel functions, were not integer multiples of the operating frequency. Since rectifying diodes produce harmonics that are integer multiples, the circular patches operated as inherent harmonic rejection filters. Additionally, dual polarization allowed for the transmit array and rectenna array to be rotated with respect to each other while maintaining stable DC power at the output of the rectenna array. MILAX functioned at 2.411 GHz [177], and ETHER's rectenna array operated at 2.45 GHz. The ETHER rectenna array was 2.7 m × 3.4 m (1200 elements) and outputted 2.8 kW. Each of ETHER's rectenna subarray panels consisted of 20 elements, received an incident power density of 850 W/m^2, and produced RF-to-DC efficiencies of 81% [178].

C. CIRCULAR POLARIZATION

In 2002, Texas A&M University developed the printed CP rectenna array shown in Fig. 37 [179]. The array used a MA/COM MA4E1317 Schottky diode and a chip capacitor to achieve 78% RF-to-DC conversion for an incident power density of 8 mW/cm^2 at 5.61 GHz. Each rectenna, placed $\lambda_0/4$ above a ground plane, used two rhombic loops which provided circularly polarization, giving them about 3 dB higher gains than traditional dipole antennas. The structure of the loops was easily integrated into CPS combining circuitry. This type of CP radiator allows for a rectenna array to have 4x fewer elements over its planar surface versus an equivalently sized LP array, albeit at the expense of a reduced field of view, due to the increase antenna element directivity. In a 1979 paper [180], researchers at General Electric Co. had estimated that an SPS-system terrestrially located rectenna array, slated for a certain proposed architecture, would need around 13 billion low-gain receiving elements and 7 billion rectifiers. The rectifying diodes alone for such an array were estimated to cost $298 million in 1979 dollars. Cutting the number of diodes by 4x would be a significant savings.

In 2001, the University of Colorado, Boulder, CO introduced two wideband rectenna arrays, seen in Fig. 38 [181]. The grid rectenna array operated from 4.5 to 8 GHz and had a maximum RF-to-DC conversion efficiency of 35% at 5.7 GHz for an incident CP power density of 7.78 mW/cm^2. The spiral array operated from 8.5 to 15 GHz and used alternating RHCP and LHCP spirals to achieve a maximum RF-to-DC conversion efficiency of 45 % at 10.7 GHz for 1.56 mW/cm^2.

D. VARIABLE LOADING

Power density variability on the surface of a rectenna array degrades the overall RF-to-DC conversion efficiency if loading over the array remains constant. This was shown in the 1974 JPL tests. In 2013, Chinese researchers at the Sichuan University in Chengdu, China revisited this issue looking at a way to simplify variable loading for increased efficiency. To do so, they built the connectorized rectenna array shown in Fig. 39. The 0.5 m × 0.5 m array had 72 rectenna elements arranged along a $\lambda_0/2$ equilateral triangular lattice. Two loading schemes were used for testing when the 16-dB transmitting horn antenna was 12.2 cm away from the rectenna array. The move to the two-resistor topology resulted in RF-to-DC conversion efficiencies that were 5% higher [182].

E. TRANSPARENCY

Transparency is another desirable characteristic that could enable rectennas to better integrate into urban environments, or to prevent shadowing of the sun in large-scale installations. In 2014, French researchers developed the Fig. 40 array printed

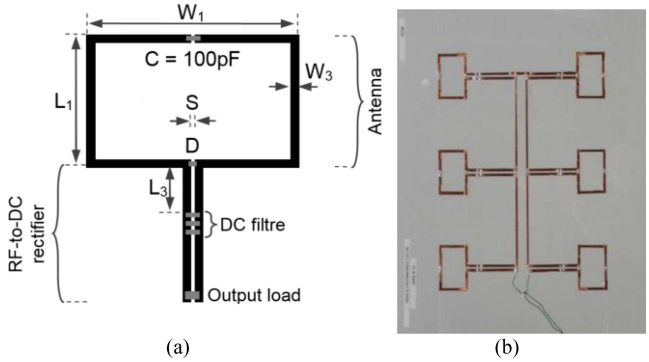

FIGURE 40. Transparent rectenna array: (a) single element layout and (b) manufactured array.

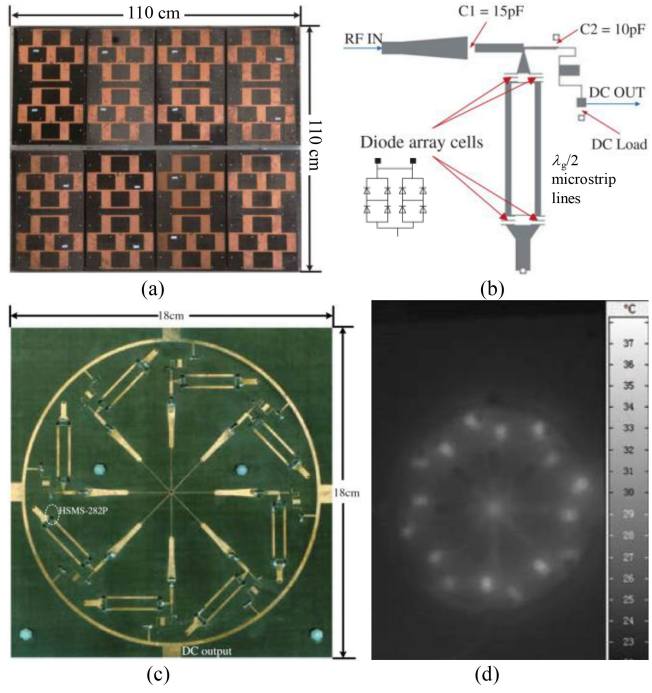

FIGURE 41. Sichuan University design for temperature stability: (a) 16 element array, (b) rectifier circuit layout, (c) 8-rectifier radial circuit, and (d) temperature distributon.

on transparent plexiglass. This array used six loop antennas with each having a coplanar stripline RF-to-DC rectifier. DC voltages of 70 and 190 mV were measured for incident power densities of 1 and 5 μW/cm^2, respectively [183].

F. ARRAY CONSIDERATIONS AT HIGH POWER

In 2015, researchers at Sichuan University built the Fig. 41 rectenna array to handle powers greater than 10 W while maintaining temperature stability. The 1-m^2 rectenna array, designed to operate at 2.45 GHz, is shown in Fig. 41(a). It used eight microstrip grid array antennas for power collection. The rectifier circuit layout, shown in Fig. 41(b), used half-wavelength branches to separate the two diode sites in order

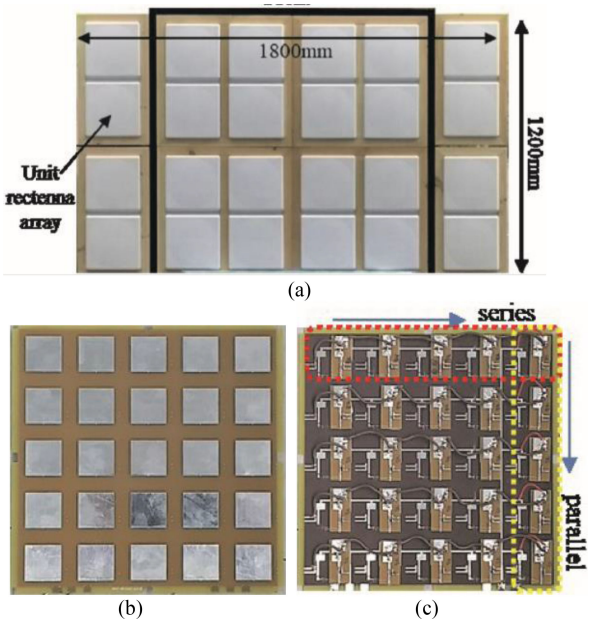

FIGURE 42. Korean 100 W 2.45 GHz rectenna array: (a) full array, (b) 5 × 5 patch antennas (front), and (c) 5 × 5 array of rectifiers (back).

to distribute the heat and avoid overheating. Fig. 41(c) shows the radially arranged circuit, combining eight of the rectifier branches. This circuit produced 68.1% RF-to-DC conversion at an input power around 41 dBm. The temperature distribution is seen in °C in Figure 14(d) with each site clearly visible. Each of the 8 antennas in Fig. 41(a) was equipped with the circuit seen in Fig. 41(c) for a total of 2,048 Schottky diodes. The rectenna array achieved output powers reaching 67.3 W at a distance 5.5 m from the transmitting antenna [184].

In 2018, Korean researchers once again put the focus on high power and developed the 2.45-GHz 100-W rectenna array shown in Fig. 42(a). This array was made up of 24 rectenna array panels. Each panel was a 5 × 5 rectenna array, like the one in Fig. 42(b)–c. The panels consisted of patch antennas with each patch having a designated rectifying circuit. The 2.16-m^2 paneled rectenna array, made of 600 rectenna elements, rectified enough DC power to turn on a 60-W LED bar at 10-m distance [187].

G. CMOS MMWAVE RECTENNA ARRAYS

CMOS technology has also found its way into rectenna design. CMOS becomes advantageous at shorter wavelengths where antennas can be integrated on-chip. This allows for the antenna and rectifier to be fully integrated, albeit at the expense of antenna element efficiency. In 2017, researchers at Tel Aviv University introduced their 95 GHz energy harvesting rectenna array system seen in Fig. 43(a). It consisted of a 3 × 3 array of 65-nm CMOS rectennas on a PCB. A peripheral connector was used to access the DC, and a potentiometer was present to adjust the rectenna loading. Each rectenna had a ring antenna paired in CMOS to a rectifier as shown in Fig. 43(b). The 0.611 mm^2 3 × 3 rectenna array collected

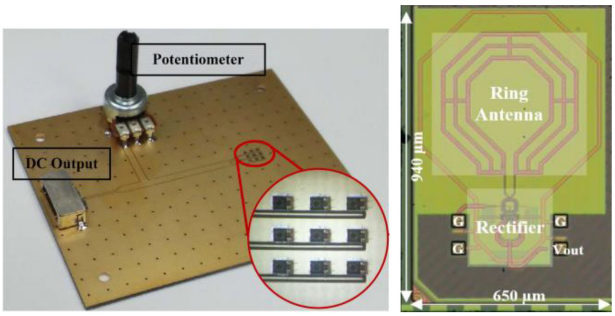

FIGURE 43. Tel-Aviv University W-band rectenna: (a) 3 × 3 rectenna system and (b) CMOS antenna/rectifier.

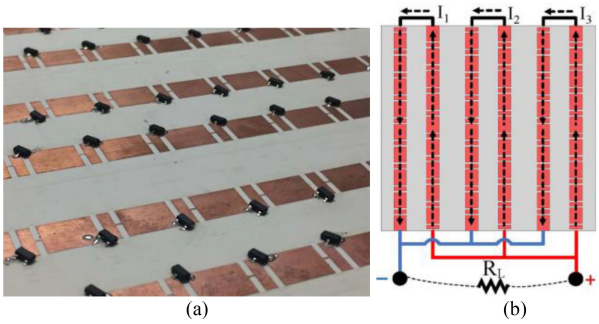

FIGURE 44. University of Waterloo/Prince Sattam University rectifying array.

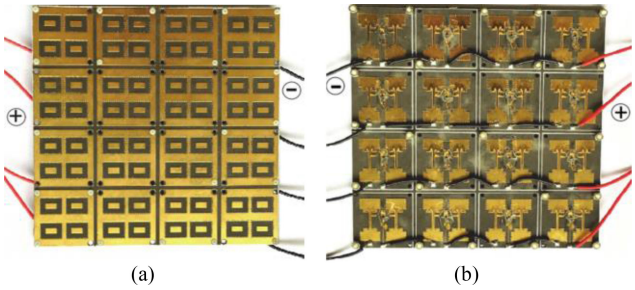

FIGURE 45. (a) Front and (b) back of the Shanghai University 35 GHz rectenna array,

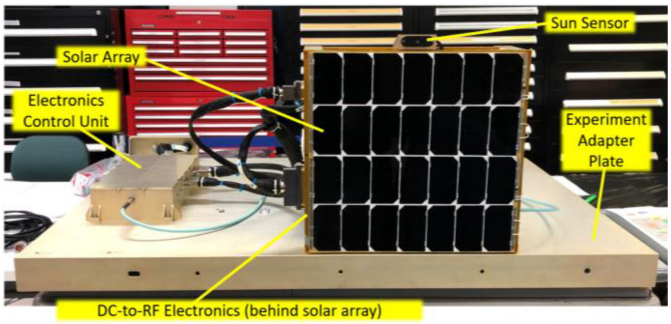

FIGURE 46. Overview of the major components of the Photovoltaic Radiofrequency Antenna Module Flight Experiment.

2.5 mW, resulting in 6% RF-to-DC conversion efficiency at 95 GHz. An individual rectifier produced 21.5% conversion at around 87 GHz for an incident power of 18.6 mW [185].

H. INCREASED AREAL ABSORPTION PER DIODE

In 2018, the University of Waterloo and Prince Sattam University collaborated on ways to increase the absorption efficiency per unit area to near unity in order to channel more RF to the rectifying diodes. Using detailed Floquet analysis, they designed the 3.4 GHz energy harvesting rectenna array shown in Fig. 44. This array used asymmetric dipoles covered by a high-permittivity TMM-10i superstrate to increase the incident power delivered to the diodes. An overall array RF-to-DC conversion efficiency of 76% was obtained experimentally, which the authors claim is the highest ever recorded for an energy harvesting surface [186].

I. BROAD BANDWIDTH, MMWAVE OPERATION

Many of the past rectenna array designs have used narrowband radiators. In 2019, Shanghai University researchers developed a novel 35 GHz millimeter-wave rectenna designed for broadband performance. The array seen in Fig. 45 was composed of 16 subarrays. Each subarray had a 2 × 2 array of slot coupled patch antennas backed by substrate integrated waveguide (SIW) cavities and a single rectifier. The antennas worked well from 31 to 40 GHz. Each 2 × 2 rectenna subarray had an RF-to-DC conversion efficiency of 51% when 13 dBm was incident upon a 550 Ω load [188].

J. FUTURE WORK

In the authors' opinion, the progress and creativity highlighted in rectenna array technologies highlighted in this section shows sufficient maturity for new work to being on productization of the technology for low cost, environmental resiliency, and compatibility with real-world power systems in support of future large-scale infrastructure and other real-world deployments.

VI. NEW DEVELOPMENTS IN POWER BEAMING TRANSMITTER TECHNOLOGIES

This section highlights new US developments in microwave and mmWave power beaming transmitters, including an in-orbit power-beaming sandwich module demonstration, three US prototypes in development for launch, and an inherently safe mmWave high power source.

A. FIRST IN-ORBIT DEMONSTRATION OF A SPACE SOLAR SANDWICH MODULE

NRL's Photovoltaic Radiofrequency Antenna Module Flight Experiment (PRAM-FX) is the first test in orbit of an element for sandwich module space solar architectures [124]. An overview of the major experiment components is shown in Fig. 46.

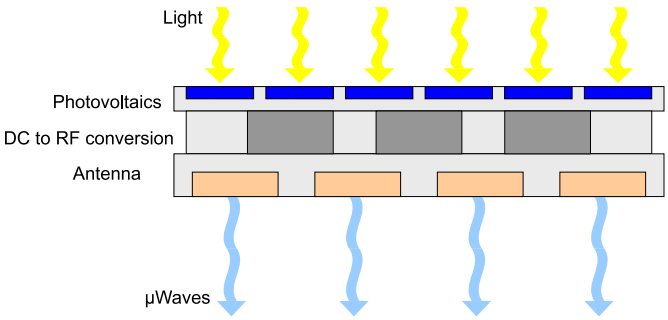

FIGURE 47. Functional depiction of a sandwich module for solar power satellites [189].

TABLE 4 Preliminary Data from PRAM-FX

Parameter	Description
Solar Constant	1321.5 W/m^2
Angle From Zenith	32°
Solar Flux Available For Collection At Angle	1120.7 W/m^2
Power Available for Collection on Solar Array	104.1 W
Solar Array Power Generated	23.5 W
Solar Array Efficiency	22.6%
RF Power Generated	8.4 W
DC-to-RF Conversion Efficiency	37.1%
Total Sandwich Module Efficiency	8.0%

The sandwich module approach to space solar is intended to reduce system mass and allow for mass production of modularized components. A sandwich module is comprised of the three layers: photovoltaics, RF Conversion, and antenna, as seen in Fig. 47.

The photovoltaics layer utilizes Spectrolab UTJ triple junction solar cells, mounted on a 30.5 cm × 30.5 cm × 1.2 cm aluminum honeycomb panel. The RF conversion layer is comprised of a power distribution board and basic off-the-shelf commercial components: a Mini-Circuits ZX95-2755+ 2.45 GHz voltage controlled oscillator, Weinschel 13-dB attenuator, Hittite HMC755LP4E driver stage amplifier, and a Cree CGH27015 final stage amplifier. The RF electronics are mounted on an aluminum honeycomb identical to the photovoltaics layer. The antenna portion of the sandwich module is omitted for this experiment due to the potential for RF interference with other experiments and general host vehicle activities. Routing the module's power output directly to an RF load for measurement also permits greater precision in measuring the power level.

Although only a very small sample of data has been received at the time of this paper's writing, preliminary indications compare quite favorably to pre-flight testing performed at NRL's Washington D.C. location. The experiment is operating in a LEO orbit that is altered throughout the course of the X-37B's mission. The experiment on occasion uses heaters to simulate the thermal environment in a Geosynchronous Orbit (GEO), where the sun would be nearly continuously shining on the solar array and thermally heating the sandwich module. The preliminary data received at this point is solely from the GEO thermal simulation data set. The maximum RF power achieved to date is 8.4 W, at an angle of 32 degrees from zenith. This corresponds a total module efficiency of approximately 8%, as seen in Table 4. Though these results are preliminary, they compare favorably with the performance documented in ground testing [190], which also demonstrated 8% total module efficiency.

As the experiment proceeds, a full picture of the module's performance under different illumination and temperature conditions in the space environment will be uncovered.

B. ORBITAL DEMONSTRATIONS FOR LARGE-SCALE DEPLOYABLE SPS

The Air Force Research Laboratory (AFRL) is executing a major demonstration project with the goal of beaming power collected in space to expeditionary forces on Earth. The motivation for this capability is clear: assured energy supply with reduced vulnerabilities and lower cost logistics. The AFRL project created to achieve this capability is Space Solar Power Incremental Demonstrations and Research (SSPIDR). SSPIDR is methodically pursuing rapid, demonstration-driven activities with increasing performance and integration level to reduce risk for an operational space solar power system. Within this construct, SSPIDR has two major thrust areas: (1) incremental demonstrations and (2) developing critical technology elements (CTEs).

The SSPIDR operational system architecture is built around the innovative concept of a modular solar-to-RF panel. Modular solar-to-RF panels will enable very large RF apertures to be assembled from a single panel design. Design objectives for the modular solar-to-RF panel include minimizing mass and enabling compact stowed packaging in the launch vehicle fairing (i.e., large deployed aperture area from small packaged volume). As such, beneficial module attributes include thinness, low mass areal density, and flexibility.

In route to achieve the ambitious goal of a full operational space power system, SSPIDR has established four distinct project demonstration phases: proof-of-principle component prototypes (Phase I), a subscale integrated prototype (Phase II), a full-scale space solar power spacecraft prototype (Phase III), and a fully operational constellation (Phase IV). Technology development work for the critical technology elements is being pursued in parallel to these prototype demonstrations to enable a more advanced prototype for the next phase, as illustrated in Fig. 48. For Phase I, key technologies will be demonstrated at various levels of integration, but still somewhat disaggregated, to increase their technology readiness levels (TRL) for the next phase. The relatively low project entry TRLs of these key technologies motivated this approach to ensure that the success of one experiment (demonstration) was not overly dependent on the success of other experimental, low TRL technologies.

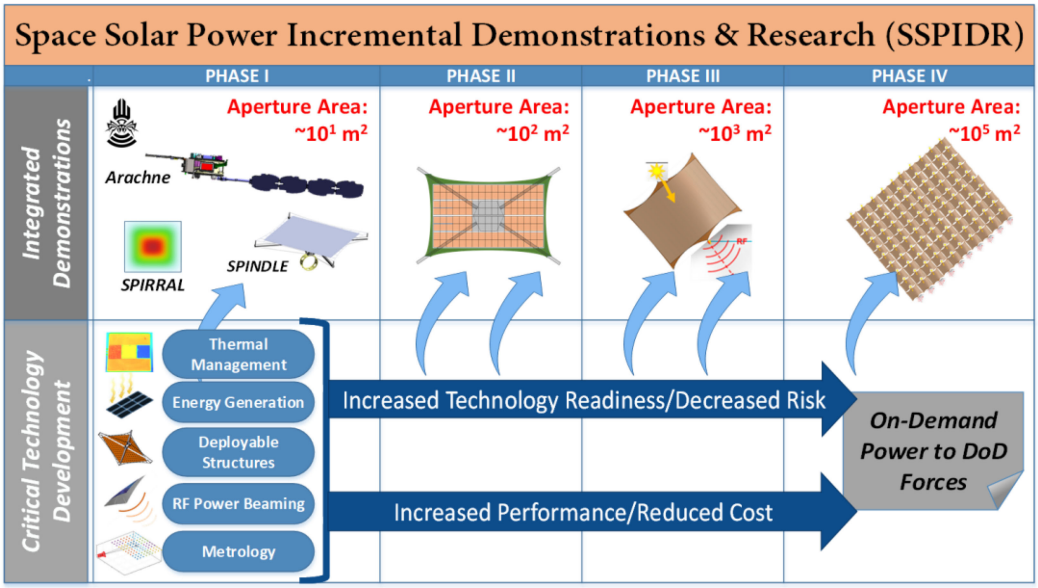

FIGURE 48. SSPIDR project phases.

Three initial in-orbit prototype demonstrations are being developed in Phase I to advance the TRL of the needed component technologies to enable an operational space solar power system. These demonstrations include: (1) Arachne, (2) SPINDLE, and (3) SPIRRAL. Arachne will be the world's first space-to-ground power beaming demonstration of a solar-to-RF modular panel with in-situ surface-shape measurement to optimize beam formation. The solar-to-RF panel technology is designed to scale to very large apertures and to support high volume, low-cost manufacturing. Arachne is planned to fly in 2023. SPINDLE will test on-orbit structural deployment of a sub-scale version of the operational system. SPINDLE is designed to test deployment kinematics and deployed structural dynamics. Finally, SPIRRAL will test thermal management approaches to ensure a long-lasting, high-performance system. The SPIRRAL experiment is planned to launch in 2023 via Alpha Space's MISS-E platform for rendezvous with the International Space Station.

To ensure the space power system achieves high performance, multiple critical technology elements (CTEs) require development and maturation. These include thermal management, energy generation, deployable structures, RF power beaming, and surface metrology (shape measurement). Parallel research and development efforts are underway in each of these areas to identify and mature successful technology approaches such that the objective system performance can be achieved. For example, packaging in a mass and volume efficient way is more achievable if the deployed structure is not required to enforce relative antenna positioning. To enable this, in-situ metrology (surface shape measurement) approaches are being developed for effective RF beam formation. Research to develop deployable structures that can produce very large area apertures from very compact stowed volumes is ongoing with several industry partners. As an example of a CTE in development for SSPIDR, Fig. 49 illustrates a 1-m^2 rectenna array developed by NRL to rectify very low incident powers in the 1–1000 mW/m^2 range for Arachne and other early demonstrations.

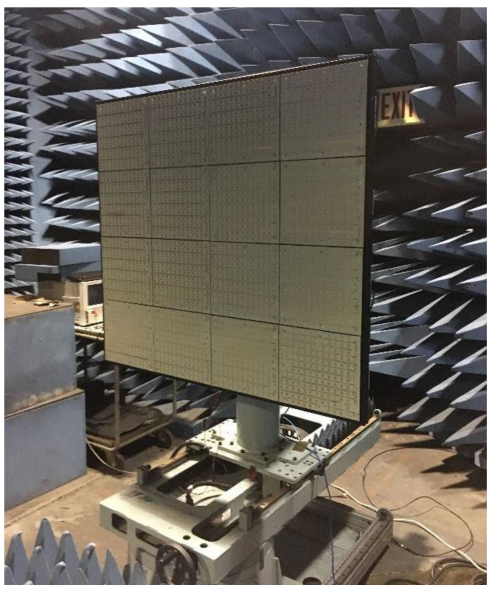

FIGURE 49. Rectenna demonstration targeting high efficiency at low incident power densities for early SSPIDR demonstrations of space-to-earth power beaming.

Additional challenges for a fully operational space power system are system cost and end-to-end efficiency. Addressing these challenges requires reducing solar cell costs while maintaining or even increasing solar-to-DC conversion efficiency.

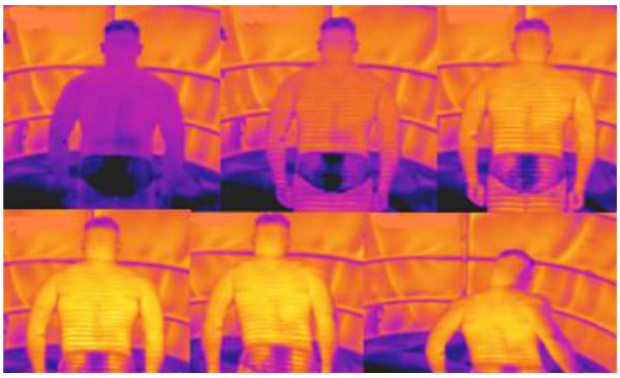

FIGURE 50. Millimeter wave radiation is absorbed by the human skin (0.4-mm thickness) resulting in instant heating as shown in the IR pictures when the back of a target person is radiated (max. effect bottom right). It is uncomfortable but safe and completely reversible in its effects.

It also requires advanced RF integrated circuits with high efficiency at expected operating conditions. Solar cell and RF integrated circuit technology development is underway that is addressing both of these challenges with both industry and government laboratory partners.

C. HIGH POWER MMWAVE TRANSMITTERS DEMONSTRATE INHERENT HUMAN SAFETY

Raytheon is developing power beaming as a dual-use capability for mmWave "active denial" directed energy systems. Such systems were developed beginning the early 90s for use as non-lethal weapons [191]–[193]. Since mmWave penetration of human skin at 95 GHz is constrained to only 0.4-mm, there is potential for active denial systems to provide inherent safety to humans inadvertently exposed to the beam.

The infrared time-capture image in Fig. 50 illustrates this effect. As power density rises, the radiation generates a heating sensation on the skin, reaching an intolerable effect that forces a repel response from the target. The beam spot size, location, duration, and intensity are controlled carefully for the desired effect. It is completely reversible and no damage occurs on the skin when the non-lethal operational protocol is observed. The systems have been on trial for more than two decades, with extensive data collected on various targets and many safety features incorporated.

For power beaming applications, the ability to control beam spot size and power density can be used to direct power at mmWave rectenna panels [195]. Having control over the performance criteria of the transmitter allows for tight specification of the rectenna design in order to maximize conversion efficiency for the overall power beaming system. Two transmitters are shown in Fig. 51. A 100 kW gyrotron transmitter [192] is used for power beaming at ranges of about 1 km, and a 7 kW solid state transmitter [193]–[195] targets <500 m applications. The solid-state transmitter is a more compact, pallet-based system that can be incorporated onto a variety of platforms. The design includes all associated components such as the array modules, transmitter assembly, thermal management and battery pack for continuous operation. Unique applications under consideration include remote wireless charging for low size, weight and power systems in dense urban environments—e.g., proximity and situational awareness sensors.

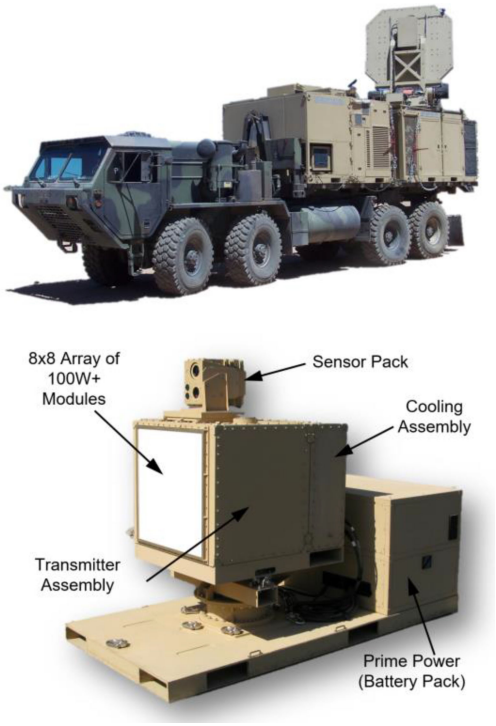

FIGURE 51. The 100 kW gyrotron (top) and 7 kW solid-state (bottom) mmWave transmitters used for dual capability of active denial and power beaming.

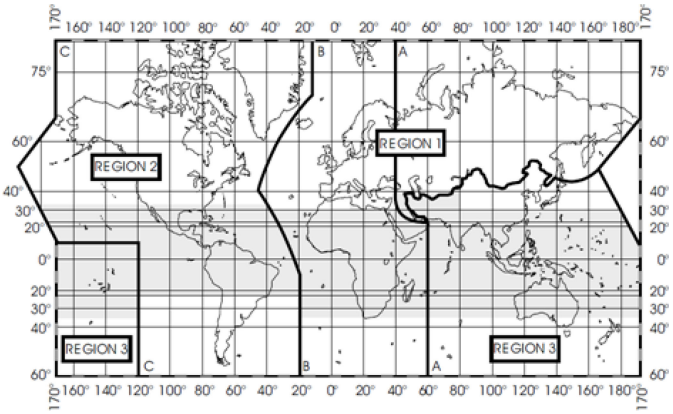

FIGURE 52. The three ITU regions [196].

VII. REGULATORY CONCERNS

A. SPECTRUM

For the past 50 years, 2.45 and 5.8 GHz have been the most popular frequencies for power beaming demonstrations and

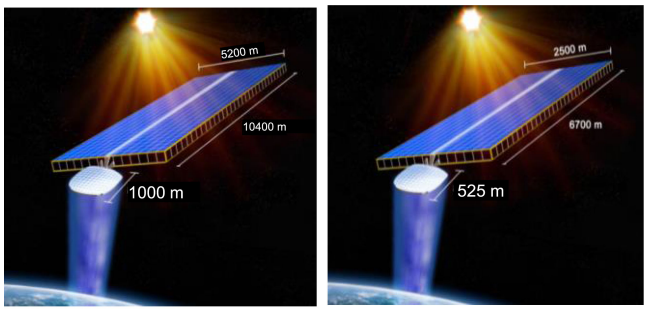

FIGURE 53. (a) 2.45-GHz NASA Reference System [197]. (b) 5.8 GHz Solar High design [198].

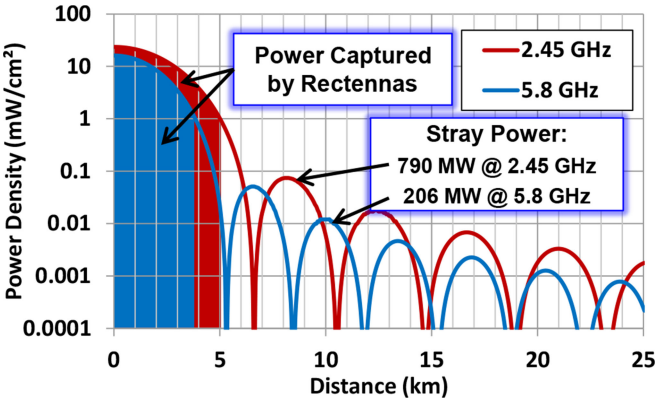

FIGURE 54. Close-in power patterns at the Earth's surface.

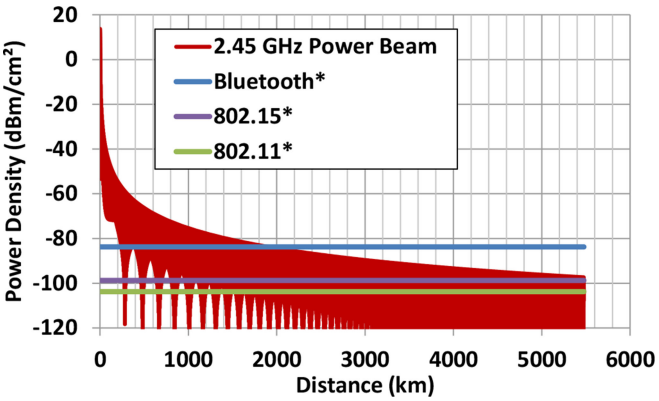

FIGURE 55. 2.45 GHz NASA Reference System radiation pattern and device sensitivities. The "∗" indicates an assumption that the receiving radio antenna has a 0 dBi gain.

technology development. Both frequencies reside in the center of an Industrial, Scientific, and Medical (ISM) frequency band. ISM bands were established for non-communication purposes such as microwave heating. However, the ISM bands have been invaded by the ever-increasing demand for communication spectrum for wireless applications. More recently, power beaming activities have been increasing at 10 GHz where 1) the aperture sizes are smaller aperture size than at

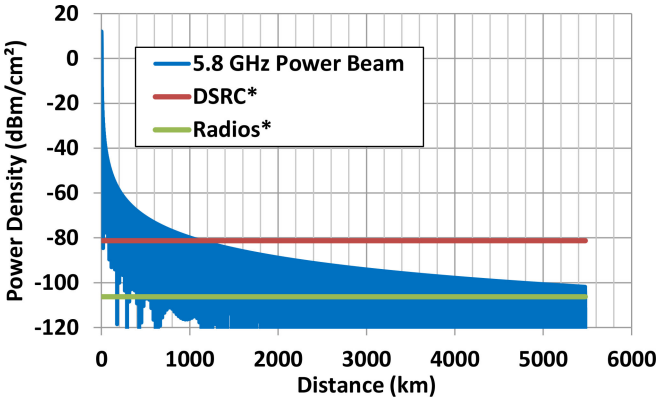

FIGURE 56. Solar High 5.8 GHz radiation pattern and device sensitivities. The "∗" indicates an assumption that the receiving radio antenna has a 0 dBi gain.

2.45 and 5.8 GHz and 2) atmospheric losses are still very low. mmWave frequencies used for power beaming technology development include the 35-GHz and 94-GHz mmWave bands, as discussed in Section II(B). Nonetheless, in spite of the many years of power beaming demonstrations and development, there does not exist a regulatory definition of power beaming services. To illustrate the challenges involved, this section focuses on spectrum issues at 2.45 and 5.8 GHz.

1) REGULATORY BODIES

Founded in 1865 to facilitate international connectivity in communications networks, the International Telecommunication Union (ITU) allocates global radio spectrum and satellite orbits and develops technical standards to ensure networks and technologies seamlessly interconnect. It divides the Earth into the three geographic regulatory regions shown in Fig. 52 and allocates frequencies into Primary and Secondary Services. Secondary Service stations cannot cause harmful interference to stations of Primary Services, and cannot claim protection from harmful interference from stations of a Primary Service, but can claim protection from harmful interference from other Secondary Services. Frequency coordination and service definition is a worldwide activity, and power beaming frequencies will need to be identified due to their high power levels compared to communication signal levels.

In addition to the ITU, each country has its own agencies for regulating spectrum. In the United States, the Federal Communications Commission (FCC) and the National Telecommunications and Information Administration (NTIA) regulate the spectrum for commercial and federal applications, respectively. Table 5 shows the 2.45 GHz and 5.8 GHz ISM bands and the services defined by the FCC and NTIA [196]. In addition to the ISM equipment, many services share the same bands. Communication devices operating in the ISM bands do not require a FCC license to operate, however they must not interfere with other devices operating in the same band. The non-interference constraint in these spectrally

TABLE 5 ISM Band Services Identified by the FCC and NTIA

ISM Band	FCC and NTIA Services
2.45 GHz ±50 MHz	ISM Equipment, Amateur Radio, Fixed Microwave, Radiolocation, Private Land Mobile, Public Safety Radio, TV Auxiliary Broadcasting, Satellite Communications, Wireless Communications
5.8 GHz ±75 MHz	ISM Equipment, RF Devices, Amateur Radio, Private Land Mobile, Personal Radio, Amateur Radio, Satellite Communications

TABLE 6 Primary Service Radio Astronomy Bands

International Bands (GHz)						US Bands (GHz)	
Region 1		Region 2		Region 3		Federal & Non-Federal	
Start	Stop	Start	Stop	Start	Stop	Start	Stop
1.4		⇨			1.427	1.4	1.427
1.6106		⇨			1.6138	1.6106	1.6138
1.66		⇨			1.67	1.66	1.67
2.69		⇨			2.7	2.69	2.7
4.99		⇨			5	4.99	5
10.6		⇨			10.7	10.68	10.7
15.35		⇨			15.4	15.35	15.4
22.21		⇨			22.5	22.21	22.5
23.6		⇨			24	23.6	24
31.3		⇨			31.8	31.3	31.8
42.5		⇨			43.5	42.5	43.5
76		⇨			77.5	76	77.5
						78	79
79		⇨			94	79	94
94.1		⇨			116	94.1	116
130		⇨			134	130	134
136		⇨			158.5	136	158.5
164		⇨			167	164	167
182		⇨			185	182	185
200		⇨			231.5	200	231.5
241		⇨			248	241	248
250		⇨			275	250	275

congested bands limits the effectiveness of power beaming applications.

In addition to power limits at the fundamental frequency, the harmonics generated from a power transmitter must be strongly filtered to avoid interfering with licensed devices operating at the harmonic frequencies. The frequencies with the most restrictive interference thresholds reside in radio astronomy (RA) bands [196]. Table 6 lists the Primary Service RA bands where there is nearly perfect alignment between ITU and United States allocations.

Receiving and converting gigawatts of microwave power into useful DC power would also impact devices with sensitive RF front ends, e.g., existing satellite receivers operating in Primary Service bands [196]. Table 7 correlates space-to-earth Primary Services for the three world-wide ITU regions and US allocations over the 1-300 GHz range. An emitter's fundamental frequency and up to its 10^{th} harmonic must be evaluated for exceeding power thresholds established by the ITU and by any affected country.

TABLE 7 Primary Service Space-to-Earth Bands

International						United States			
Region 1		Region 2		Region 3		Federal		Non-Federal	
Start	Stop	Start	Stop	Start	Stop	Start	Stop	Start	Stop
2.4835		⇨			2.5	2.4835	⇨		2.5
		2.5		⇨	2.52				
2.52		⇨			2.67				
		2.67	2.69						
3.4		⇨			4.2			3.6	4.2
4.5		⇨			4.8			4.5	4.8
5.01		⇨			5.03				
5.15		⇨			5.216	5.15	⇨		5.216
5.67		⇨			5.725				
6.7		⇨			7.075	6.7	⇨		7.075
7.25		⇨			7.85	7.25	7.85		
8.025		⇨			8.5	8.025	8.5	8.45	8.5
10.7		⇨			12.75			10.7	12.75
15.43		⇨			15.63				
17.7		⇨			21.2	17.8	21.2	18.3	20.2
21.4	22			21.4	22				
25.5		⇨			27	25.5	27		
31		⇨			31.3	31	⇨		31.3
31.8		⇨			32.3	31.8	⇨		32.3
34.7	35.2			34.7	35.2	33	36		
37		⇨			42.5	37	38	37.5	42.5
						39.5	41		
47.5	47.9								
48.2	48.5								
49.44	50.2								
71		⇨			76	71	⇨		76
123		⇨			130	123	⇨		130
158.5		⇨			164	158.5	⇨		164
167		⇨			174.5	167	⇨		174.5
232		⇨			240	232	⇨		240

TABLE 8 NASA Reference System Parameters

System Parameters		
Frequency (GHz)	2.45	
Transmitter Diameter (m)	1000	
Distance (km)	35,786	
Rectenna Diameter (m)	10000	
DC Power from Solar Collectors (MW)	8500	
System Performance		
	Efficiency	**Power (GW)**
PV-Converter-Transmitter PMAD	96%	8186
Transmitter	82%	6716
Propagation	98%	6582
RF Collection	88%	5792
Rectenna	89%	5155
Ground Rectenna-PMAD-Utility Grid	97%	**5000**
WPT DC-DC Efficiency	**58.8%**	

2) SPS ANALYSIS

To better understand potential interference situations, two representative space-to-Earth power beaming satellites are analyzed: 1) the 2.45 GHz Reference System SPS and 2) the 5.8 GHz Solar High SPS [197], [198], illustrated in Fig. 53, with design parameters shown in Tables 8 and 9. Both transmitters apply a 10 dB Gaussian amplitude taper that provides a high microwave collection efficiency at the ground rectenna, and both systems provide gigawatts of power to the utility grid. While the physical sizes are very different, the transmitter sizes are electrically similar.

PMAD = Power Management and Distribution

TABLE 9 Solar High Parameters

System Parameters		
Frequency (GHz)	5.8	
Transmitter Diameter (m)	525	
Distance (km)	35,786	
Rectenna Diameter (m)	7500	
DC Power from Solar Collectors (MW)	4410	
System Performance		
	Efficiency	**Power (GW)**
PV-Converter-Transmitter PMAD	90%	3969
Transmitter	75%	2986
Propagation	98%	2917
RF Collection	93%	2711
Rectenna	78%	2105
Ground Rectenna-PMAD-Utility Grid	95%	**2000**
WPT DC-DC Efficiency	**45.4%**	

PMAD = Power Management and Distribution

Fig. 54 shows the power density overlays at the Earth's surface on the rectennas and away from the rectenna. While the collection efficiencies are high, hundreds of megawatts of microwave power residing in thousands of sidelobes land away from the rectenna.

A further expansion of the transmitter power patterns is shown in Fig. 55 and Fig. 56. In Fig. 55, the receive power thresholds of three representative 2.45 GHz devices are shown:

- Bluetooth: −70 dBm with 3 dB of interference margin
- IEEE 802.15.4: −85 dBm with 3 dB interference margin
- IEEE 802.11: −65 to −90 dBm (data rate dependent)

These power thresholds are converted to power density with an assumed 0 dBi receive antenna gain. In all cases, the power contained in the sidelobes would degrade the sensitivities of these devices for thousands of kilometers away from the rectenna.

A similar situation exists for the 5.8 GHz Solar High SPS as seen in Fig. 56. In this case, two representative 5.8 GHz devices are selected with their minimum input power levels:

- Dedicated Short Range Communication (DSRC): −75 dBm typically with 3 dB margin
- Radios: −97 dBm typically with 3 dB margin

Again, both devices' sensitivities degrade for large distances away from the rectenna.

Finally, Table 10 compares the two power beaming frequencies and their harmonics with the RA and space-to-Earth satellite reception bands. This assessment includes a bandwidth of ±10 MHz around the power beaming frequency to account for transmitter phase noise. While the RA bands would not be impacted, the harmonics fall within space-to-Earth Primary Service bands. The transmitter's antenna would be required to filter those highlighted harmonics to non-interfering power levels. Not considered here is the potential re-radiation of harmonics from the rectenna array, as well as re-radiation of intermodulation products of other wireless signals captured by the rectenna array – all of which could also contribute to interference.

TABLE 10 Interference Assessment for Both Systems

2.45 GHz Assessment			5.8 GHz Assessment		
Harmonic No.	RA Band Freq. (GHz)	Space-to-Earth Band Freq. (GHz)	Harmonic No.	RA Band Freq. (GHz)	Space-to-Earth Band Freq. (GHz)
Fund.	2.45	2.45	Fund.	5.8	5.8
2	4.9	4.9	2	11.6	11.6
3	7.35	7.35	3	17.4	17.4
4	9.8	9.8	4	23.2	23.2
5	12.25	12.25	5	29	29
6	14.7	14.7	6	34.8	34.8
7	17.15	17.15	7	40.6	40.6
8	19.6	19.6	8	46.4	46.4
9	22.05	22.05	9	52.2	52.2
10	24.5	24.5	10	58	58

= Harmonic frequency within a Primary Service band

Because communication signal power levels are many orders of magnitude lower than power beaming levels, an inherit incompatibility exists for power beaming applications. The world's spectrum regulatory agencies have created standards to harmonize communication systems to avoid interference. Because frequencies have not been identified for power beaming services, communications infrastructure is not designed to reject these higher power signals. The analysis presented in this section illustrates the disparity.

3) FUTURE SYSTEM PROPOSALS

This section demonstrates the regulatory shortcomings of the two best-known SPS reference system designs. The lack of spectrum allocation at this advanced date in the development of microwave technology, and the high power densities involved, are significant challenges. To be realistic, future power beaming system proposals – whether terrestrial or space-based – must address the spectrum management concerns raised here. Resolution to this issue could take the form of innovative technical solutions, novel concepts of operation, and/or political agreements.

B. SAFETY

The power density manifested in a power beaming link may pose safety concerns for people, objects, and wildlife exposed to the beam. For both laser power beaming and RF power beaming, there are safety standards for limiting continuous human exposure to specific power density thresholds, as set by various organizations, including the IEEE [199], ANSI [200], and ICNIRP [201]. Limits pertain to both power density and absorbed energy, as elaborated in these documents. Power beaming systems must include measures to ensure that safety limits appropriate for a given situation are not transgressed. Novel solutions to this challenge that preserve the delivery of useful power are demonstrated in the optical regime [202]. Generally, safety systems must Detect and Decide when an unsafe situation exists, and then Defocus, Divert, Dim, or Douse the beam as appropriate; collectively, these actions are referred to as the "6 Ds."

For situations without personnel or potential vulnerable systems, power density limitations may be greatly relaxed

or effectively unconstrained. This opens a larger trade space for power beaming link and system design. However, in any circumstance, care must be taken to consider cybersecurity, physical security, and other avenues of system disruption or compromise.

VIII. CONCLUSION

This paper has defined power beaming as a distinct class of wireless power transmission, contrasting the features of microwave, mmWave, and optical modalities. Examples of beam diffraction and atmospheric loss illustrated the basic physical limits of power beaming. An in-depth review of prior results indicated recent intensification of demonstrations and activity during the last five years. An appraisal of rectenna progress to date showed sufficient maturity for new research to begin in productization and ruggedization of the technology. New results power beaming presented here include an inherently safe mmWave source, the first in-orbit demonstration of a microwave sandwich module, and the development-in-progress of three in-orbit demonstrations. Regulatory concerns, including spectrum and safety, were also addressed.

The current acceleration in microwave and mmWave power beaming activity portends a new wave of innovations and progress, enabling major opportunities in civil power distribution and baseline alternative energy, as well as new architectures for military basing [203]. Research investments in space assembly and maintenance, deployable structures, thermal management, solar energy conversion, power management, and phased array control [203] should lead to progressively increasing system capabilities, motivating the larger society to incrementally resolve economic, legal, and political challenges to widespread, large-scale adoption of this technology.

ACKNOWLEDGMENT

The authors would like to thank R. S. Darling of the Office of the Under Secretary of Defense for Research and Engineering, Arlington, VA, USA for guidance and critical review. The authors would like to thank Prof. Y. Park of KERI, Changwon, South Korea, Prof. H. Zhang of Chongqing University, Chongqing, China, Prof. B. Duan of Xidian University, Xi'an, China, Prof. C. Liu of Sichuan University, Chengdu, China, and Dr. L. Xiao of CSDDC, Wuhan, China, for providing information to Prof. N. Shinohara on recent power beaming advances in their respective regions. The authors would like to thank J. Hutson, formerly with the U.S. Naval Research Laboratory, Washington, DC, USA, for helpful technical assistance.

REFERENCES

[1] W. C. Brown, "The technology and application of free-space power transmission by microwave beam," *Proc. IEEE*, vol. 62, no. 1, pp. 11–25, Jan. 1974.

[2] B. B. Tierney and A. Grbic, "Design of self-matched planar loop resonators for wireless nonradiative power transfer," *IEEE Trans. Microw. Theory Techn.*, vol. 62, no. 4, pp. 909–919, Apr. 2014.

[3] B. Strassner and K. Chang, "Passive 5.8-GHz radio-frequency identification tag for monitoring oil drill pipe," *IEEE Trans. Microw. Theory Techn.*, vol. 51, no. 2, pp. 356–363, Feb. 2003.

[4] C. E. Baum *et al.*, "JOLT: A highly directive, very intensive, impulse-like radiator," *Proc. IEEE*, vol. 92, no. 7, pp. 1096–1109, Jul. 2004.

[5] B. Tingley, "X-37B space plane's microwave power beam experiment is a way bigger deal than it seems," May 2020. [Online]. Available: https://www.thedrive.com/the-war-zone/33339/x-37b-space-planes-microwave-power-beam-experiment-is-a-way-bigger-deal-than-it-seems

[6] Kirtland Air Force Base Public Affairs, "U.S. Air Force Research Laboratory developing space solar power beaming," Oct. 2019. [Online]. Available: https://www.robins.af.mil/News/Article-Display/Article/1998062/us-air-force-research-laboratory-developing-space-solar-power-beaming

[7] P. N. Kawashima and K. Takeda, "Laser energy transmission for a wireless energy supply to robots," *Robot. Autom. Construction*, Oct. 2008, doi: 10.5772/6194.

[8] Wi-Charge LIGHTS. Accessed: Jul. 13, 2020. [Online]. Available: https://wi-charge.com/product_category/reference-integrations

[9] W. Saad, M. Bennis, and M. Chen, "A vision of 6G wireless systems: Applications, trends, technologies, and open research problems," *IEEE Netw.*, vol. 34, no. 3, pp. 134–142, May/Jun. 2020.

[10] "Energy transmitted by laser in 'historic' power-beaming demonstration," NRL Press Release, Oct. 2019. [Online]. Available: https://www.nrl.navy.mil/news/releases/researchers-transmit-energy-laser-power-beaming-demonstration with video at https://youtu.be/Xb9THqrXd4I

[11] International Telecommunication Union, "Attenuation due to clouds and fog," Recommendation ITU-R P.840-8, Geneva, Aug. 2019.

[12] A. Grebennikov, *RF and Microwave Transmitter Design*, 1st ed. New York, NY, USA: Wiley, 2011.

[13] R. M. Dickinson and W. C. Brown, "Radiated microwave power transmission system efficiency measurements," NASA Tech. Memo, pp. 33–727, May 1975.

[14] K. D. Song *et al.*, "Preliminary operational aspects of microwave-powered airship drone," *Int. J. Micro Air Veh.*, Jan. 2019, doi: 10.1177/1756829319861368.

[15] B. Duan, "On new developments of space solar power station (SSPS) of China," in *Proc. 36th Int. Space Develop. Conf.*, St. Louis, USA, May 2017.

[16] N. Shinohara, *Beam Control Technologies With a High-Efficiency Phased Array For Microwave Power Transmission in Japan*. Kyoto, Japan: Kyoto Univ. Res. Inf. Repository, 2013.

[17] W. C. Brown, "The history of the development of the rectenna," in *SPS Microwave Systems Workshop*. Houston, TX, USA: Lyndon B. Johnson Space Center, Jan. 1980.

[18] "Ground demonstration testing of microwave wireless power transmission," JAXA Res. Develop. Directorate. Accessed: Jul. 9, 2020. [Online]. Available: http://www.kenkai.jaxa.jp/eng/research/ssps/150301.html

[19] R. M. Dickinson and O. Maynard, "Ground based wireless and wired power transmission cost comparison," in *Proc. Int. Energy Convers. Eng. Conf. (IECEC)*, Vancouver, Canada, Aug. 1999. Accessed: Apr. 25, 2020. [Online]. Available: http://hdl.handle.net/2014/17841

[20] J. J. Schlesak, A. Alden, and T. Ohno, "A microwave powered high altitude platform," in *Proc. IEEE Int. Microw. Symp.*, 1988, pp. 283–286.

[21] B. Duan, "On new developments of space solar power station (SSPS) of china," in *Proc. 36th Int. Space Develop. Conf.*, St. Louis, USA, May 25, 2017.

[22] R. M. Dickinson, "Wireless power transmission technology state of the art the first Bill Brown lecture," *Acta Astronautica*, vol. 53, no. 4, pp. 561–570, 2003.

[23] *Transmitting Power Without Wires*, Bang Goes the Theory - Series 6, Episode 5, BBC One, College Park, MD, USA, May 22, 2012. [Online]. Available: https://www.bbc.co.uk/programmes/p00yjt99

[24] T. J. Nugent, Jr., D. Bashford, T. Bashford, T. J. Sayles, and A. Hay, "Long-range, integrated, safe laser power beaming demonstration," in *Proc. Opt. Wireless Fiber Power Transmiss. Conf. (OWPT)*, Yokohama, Japan, Apr. 2020, pp. 12–13.

[25] T. He *et al.*, "High-power high-efficiency laser power transmission at 100m using optimized multi-cell gaas converter," *Chin. Phys. Lett.*, vol. 31, no. 10, pp. 1042031–1042035, 2014.

[26] R. Akiba, K. Miura, M. Kinada, H. Matsumoto, and N. Kaya, "ISY-METS rocket experiment," Inst. Space Astronaut. Sci. Rep., ISSN 0285-6808, 1993.

[27] T. Nugent, "Review of laser power beaming demonstrations by powerlight technologies (formerly lasermotive)," in *Proc. Directed Energy Sci. Technol. Symp.*, Oxnard, CA, USA, Feb. 2018.

[28] T. Talbert, "NASA - LaserMotive LLC wins prize in power beaming challenge." Accessed: Nov. 10, 2009. [Online]. Available: https://www.nasa.gov/offices/oct/early_stage_innovation/centennial_challenges/cc_pb_feature_11_10_09.html

[29] J. E. Degenford, M. D. Sirkis, and W. H. Steier, "The reflecting beam waveguide," *IEEE Trans. Microw. Theory Techn.*, vol. 12, no. 4, pp. 445–453, Jul. 1964.

[30] P. L. Heron, G. P. Monahan, J. W. Mink, F. K. Schwering, and M. B. Steer, "Impedance matrix of an antenna array in a quasi-optical resonator," *IEEE Trans. Microw. Theory Techn.*, vol. 41, no. 10, pp. 1816–1826, Oct. 1993.

[31] J. C. McCleary, "Studies on beam propagation pertaining to beamed microwave power transmission and open resonator quasi-optics," Master's thesis, Dept. Elect. Eng., Texas A&M Univ., College Station, TX, USA, 1991.

[32] R. C. Hansen, J. McSpadden, and J. N. Benford, "A universal power transfer curve," *IEEE Microw. Wireless Compon. Lett*, vol. 15, no. 5, pp. 369–371, May 2005.

[33] P. F. Goldsmith, "Quasi-optical techniques," *Proc. IEEE*, vol. 80, no. 11, pp. 1729–1747, Nov. 1992.

[34] *IEEE Standard for Definitions of Terms for Antennas*, IEEE Std 145-2013, pp. 1–50, 6 Mar. 2014.

[35] T. Uno, and S. Adachi, "Optimization of aperture illumination for radio wave power transmission," *IEEE Trans. Antennas Propag.*, vol. 32, no. 6, pp. 628–632, Jun. 1984.

[36] A. Massa, G. Oliveri, F. Viani, and P. Rocca, "Array designs for long-distance wireless power transmission: State-of-the-art and innovative solutions," *Proc. IEEE*, vol. 101, no. 6, pp. 1464–1481, Jun. 2013.

[37] S. Silver, *Microwave Antenna Theory and Design*. New York, NY, USA: McGraw-Hill, 1949.

[38] J. Hutson, and C. T. Rodenbeck, "Computation of microwave power beaming efficiency, with application to amplitude and phase optimization," NRL Rep., in review for public release.

[39] J. Kiefer, "Sequential minimax search for a maximum," *Proc. Amer. Math. Soc.*, vol. 4, no. 3, pp. 502–506, Feb. 1953.

[40] R. L. Lewis, and A. C. Newell, "Efficient and accurate method for calculating and representing power density in the near zone of microwave antennas," *IEEE Trans. Antennas Propag.*, vol. 36, no. 6, pp. 890–901, Jun. 1988.

[41] J. T. Logan, D. S. Reinhard, and K. E. Hauck, "Phased array calibration and diagnostics utilizing a student-built planar near-field system," in *Proc. IEEE Int. Symp. Phased Array Syst. Technol.*, Oct. 2010, pp. 279–286.

[42] L. Z. Pazin, "Field of a circular aperture antenna in the fresnel diffraction region," *J. Commun. Technol. Electron.*, vol. 41, no. 15, 1996, transl. *Radiotekhnika i Elektronika*, vol. 41, no. 12, 1996, pp. 1468–1470.

[43] T. A. Cott, "RF radiation over millstone hill," MIT Lincoln Lab. Tech. Rep. 1141, Dec. 2009.

[44] International Telecommunication Union, "The radio refractive index: Its formula and refractivity data," Recommendation ITU-R P.453-14, Geneva, Aug. 2019.

[45] International Telecommunication Union, "Reference standard atmospheres," Recommendation ITU-R P.835-6, Geneva, Dec. 2017.

[46] R. A. Minzner *et al.*, "Defining constants, equations, and abbreviated tables of the 1975 U.S. standard atmosphere," NASA TR R-459, Washington, DC, May 1976.

[47] International Telecommunication Union, "Attenuation by atmospheric gases and related effects," Recommendation ITU-R P.676-12, Geneva, Aug. 2019.

[48] H. J. Liebe, "An updated model for millimeter wave propagation in moist air," *Radio Sci.*, vol. 20, no. 5, pp. 1069–1089, Sep./Oct. 1985.

[49] International Telecommunication Union, "Specific attenuation model for rain for use in prediction methods," Recommendation ITU-R P.838-3, Mar. 2005.

[50] J. Hutson and C. T. Rodenbeck, "Computational model for atmospheric propagation losses at radiofrequency and millimeter wave frequencies," NRL Rep., in review for public release.

[51] R. M. Dickinson and W. C. Brown, "Radiated microwave power transmission system efficiency measurements," Jet Propulsion Lab., Tech. Rep. NASA-CR-142986, JPL-TM-33-727, May 1975.

[52] P. Jaffe and J. McSpadden, "Energy conversion and transmission modules for space solar power," *Proc. IEEE*, vol. 101, no. 6, pp. 1424–1437, Jun. 2013.

[53] R. M. Dickinson, "Ground based wireless and wired power transmission cost comparison," in *Proc. Int. Energy Convers. Eng. Conf. (IECEC)*, Aug. 1999.

[54] A. B. W. Kennedy and H. R. Sankey, "The thermal efficiency of steam engines," Report of the Committee Appointed to the Council Upon the Subject of the Definition of a Standard or Standards of Thermal Efficiency for Steam Engines, Jan. 1898.

[55] W. C. Brown, "The history of power transmission by radio waves," *IEEE Trans. Microw. Theory Techn.*, vol. 32, no. 9, pp. 1230–1242, Sept. 1984.

[56] B. Strassner and K. Chang, "Microwave power transmission: Historical milestones and system components," *Proc. IEEE*, vol. 101, no. 6, pp. 1379–1396, Jun. 2013.

[57] M. Cheney, *Tesla, Man Out of Time*. Englewood Cliffs, NJ, USA: Prentice-Hall, 1981.

[58] J. F. Showron, G. H. MacMaster, and W. C. Brown, "The super power CW amplitron," *Microw. J.*, Oct. 1964.

[59] R. H. George and E. M. Sabbagh, "An efficient means of converting microwave energy to dc using semiconductor diodes," *IEEE Trans. Microw. Theory Techn.*, vol. 11, no. 3, pp. 132–141, Mar. 1963.

[60] W. C. Brown, "Thermionic diode rectifier," in *Microwave Power Engineering*, I. E. C. Okress, Ed. New York, NY, USA: Academic, 1968, pp. 295–298.

[61] W. C. Brown, "The history of the development of the rectenna," in *Proc. Rectenna Session SPS Microw. Syst. Workshop*, Jan. 15–18, 1980.

[62] R. H. George, "Solid-state power rectifications," *Microw. Power Eng.*, vol. 1, pp. 275–294, 1968.

[63] W. C. Brown, R. H. George, N. I. Heenan, and R. C. Wonson, "Microwave to DC converter," U.S. Patent 3,434,678, 1969.

[64] W. C. Brown, "Experimental airborne microwave supported platform," Tech. Rep. RADC-TR-65-188, Contract AF30 (602) 3481, Dec. 1965.

[65] P. Glaser, "Power from the sun: Its future," *Sci. Mag.*, vol. 162, no. 3856, pp. 857–861, Nov. 1968.

[66] P. E. Glaser, F. P. Davidson, and K. I. Csigi, *Solar Power Satellites*. New York, NY, USA: Wiley, 1994.

[67] P. D. Potter, "A new horn antenna with suppressed sidelobes and equal beamwidths," *Microw. J.*, vol. 6, pp. 71–78, 1963.

[68] W. C. Brown, "Free-space microwave power transmission study," Combined Phase III Final Rep., Raytheon Rep. PT-4601, NASA Contract NAS-8-25374, Sep. 1975.

[69] W. C. Brown, "Satellite power stations – A new source of energy?" *IEEE Spectr.*, vol. 10, no. 3, pp. 38–47, Mar. 1973.

[70] R. M. Dickinson and W. C. Brown, "Radiated microwave power transmission system efficiency measurements," Tech. Memo 33-727, Jet Propulsion Lab, California Inst. Technol., Mar. 15, 1975.

[71] R. M. Dickinson, "Evaluation of a microwave high-power reception-conversion array for wireless power transmission," Tech. Memo 33-741, Jet Propulsion Lab., California Inst. Technol., Sep. 1, 1975.

[72] R. M. Dickinson, "Reception-conversion subsystem (RXCV) transmission system," Raytheon Final Rep. Microw. Power, ER75-4386, JPL Contract 953968, NASA Contract NAS 7-100, Sep. 1975.

[73] *Final Proc. Solar Power Satellite Program Rev. DOE/NASA Satellite Power System Concept Develop. Evaluation Program*, Conf.-800491, Jul. 1980.

[74] J. Schlesak, A. Alden, and T. Ohno, "SHARP rectenna and low altitude flight trials," in *Proc. IEEE Glob. Telecommun. Conf.*, Dec. 2–5, 1985.

[75] H. Matsumoto, "Microwave power transmission," *J. Aerosp. Soc.*, vol. 32, pp. 120–127, 1989.

[76] Y. Fujino *et al.*, "A rectenna for MILAX," in *Proc. Wireless Power Transmiss. Conf.*, Feb. 1993, pp. 273–277.

[77] H. Matsumoto, N. Kaya, I. Kimura, S. Miyatake, M. Nagatomo, and T. Obayashi, "MINIX project toward the solar power satellite-rocket experiment of microwave energy transmission and associated nonlinear plasma physics in the ionosphere," in *Proc. ISAS Space Energy Symp.*, 1982, pp. 69–76.

[78] M. Nagatomo, N. Kaya, and H. Matsumoto, "Engineering aspect of the microwave ionosphere nonlinear interaction experiment (MINIX) with a sounding rocket," *Acta Astronautica*, vol. 13, no. 1, pp. 23–29, 1986.

[79] R. Akiba, K. Miura, M. Hinada, H. Matsumoto, and N. Kaya, "ISY-METS rocket experiment," *Inst. Space Astronaut. Sci.*, no. 652, pp. 1–13, 1993.

[80] J. Hawkins, S. Houston, M. Hatfield, and W. Brown, "The SABER microwave-powered helicopter project and related WPT research at the university of Alaska Fairbanks," in *AIP Conf. Proc.*, vol. 420, pp. 1092–1097, 1998.

[81] N. Shinohara and H. Matsumoto, "Dependence of DC output of a rectenna array on the method of interconnection of its array elements," *Elect. Eng. Jpn.*, vol. 125, no. 1, pp. 9–17, 1998.

[82] N. Kaya, S. Ida, Y. Fujino, and M. Fujita, "Transmitting antenna system for airship demonstration (ETHER)," *Space Energy Transp.*, vol. 1, no. 4, pp. 237–245, 1996.

[83] H. Matsumoto, "Research on solar power satellites and microwave power transmission in Japan," *IEEE Microw. Mag.*, vol. 3, no. 4, pp. 36–45, Dec. 2002.

[84] A. Celeste, P. Jeanty, and G. Pignolet, "Case study in Reunion Island," *Acta Astronautica*, vol. 54, no. 4, pp. 253–258, Feb. 2004.

[85] R. Nansen, *Sun Power*. Ocean Shores, WA, USA: Ocean Press, 1995.

[86] Y. Park, private communication, Korea Electrotechnol. Res. Inst. (KERI).

[87] J. M. Mcspadden and J. C. Mankins, "Summary of recent results from NASA's space solar power (SSP) programs and the current capabilities of microwave WPT technology," *IEEE Microw. Mag.*, vol. 3, pp. 46–57, Dec. 2002.

[88] B. Strassner and K. Chang, "5.8 GHz circularly polarized dual rhombic loop traveling wave rectifying antenna for low power density wireless power transmission applications," *IEEE Trans. Microw. Theory Techn.*, vol. 51, no. 5, pp. 1548–1553, May 2003.

[89] L. H. Hsieh *et al.*, "Development of a retrodirective wireless microwave power transmission system," in *Proc. IEEE Int. Symp. Antennas Propag.*, Jun. 2003, pp. 393–396.

[90] M. Mori, H. Kagawa, and Y. Saito, "Summary of studies on space solar power systems of Japan Aerospace Exploration Agency (JAXA)," *Acta Astronautica*, vol. 59, no. 1, pp. 132–138, Jul. 2006.

[91] N. Shinohara, H. Matsumoto, and K. Hashimoto, "Phase-controlled magnetron development for SPORTS: Space power radio transmission system," *Radio Sci. Bull.*, no. 310, Sept. 2004.

[92] H. Matsumoto *et al.*, "Experimental equipments for microwave power transmission in Kyoto University," in *Proc. 4th Int. Conf. Solar Power Space*, Jun. 30 – Jul. 2, 2004.

[93] J. Foust, "A step forward for space solar power," *The Space Review*, Sep. 15, 2008.

[94] "Solar power beamed from space within a decade?" *New Atlas*, Feb. 23, 2009.

[95] N. Shinohara, "Beam control technologies with a high-efficiency phased array for microwave power transmission in Japan," *Proc. IEEE*, vol. 101, no. 6, pp. 1448–1463, Jun. 2013.

[96] S. Sasaki, "How Japan plans to build an orbital solar farm," *IEEE Spectr.*, Apr. 24, 2014.

[97] T. Nishioka and S. Yano, "Mitsubishi heavy takes step toward long-distance wireless power," *Nikkei Asian Rev.*, Mar. 16, 2015.

[98] N. Shinohara, H. Matsumoto, and K. Hashimoto, "Solar power station/satellite (SPS) with phase controlled magnetrons," *IEICE Trans. Electron.*, vol. E86-C, no. 8, pp. 1550–1555, 2003.

[99] S. Mihara *et al.*, "The result of ground experiment of microwave wireless power transmission," in *Proc. 66th Int. Astronaut. Congr.*, 2015, Paper IAC-2015-C3.2.1.

[100] S. Mihara *et al.*, "The current status of microwave power transmission for SSPS and industry application," in *Proc. 68th Int. Astronaut. Congr.*, 2017, Paper IAC-2017-C3.2.9.

[101] N. Shinohara, N. Hasegawa, S. Kojima, and N. Takabayashi, "New beam forming technology for narrow beam microwave power transfer," in *Proc. 8th Asia-Pacific Conf. Antennas Propag. (APCAP)*, 2019.

[102] S. Mizojiri, and K. Shimamura, "Wireless power transfer via subterahertz-wave," *Appl. Sci.*, vol. 8, 2018, Art. no. 2653.

[103] S. Mizojiri *et al.*, "Demonstration of sub-terahertz coplanar rectenna using 265 GHz gyrotron," in *Proc. IEEE Wireless Power Week (WPW)*, 2019, pp. 409–412.

[104] K. Song *et al.*, "Preliminary operational aspects of microwave-powered airship drone," *Int. J. Micro Air Veh.*, vol. 11, pp. 1–10, 2019.

[105] L. Jeon, "Transmitter for high power microwave wireless power transmission (in Korean)," *Mag. Korea Inst. Elect. Eng. (KIEE)*, Sep. 2019, pp. 11–14.

[106] K. Needham, "Plans for first Chinese solar power station in space revealed," *The Sydney Morning Herald*, Feb. 15, 2019.

[107] H. Zhang, private communication, Chongqing Univ., China.

[108] Y. Dong *et al.*, "Focused microwave power transmission system with high-efficiency rectifying surface," *IET Microw., Antennas Propag.*, vol. 12, no. 5, pp. 808–813, 2018.

[109] B. Duan, private communication, Xidian Univ., China.

[110] C. Liu, private communication, Sichuan Univ., China.

[111] H. Zhang and C. Liu. "A high-efficiency microwave rectenna array based on subarray decomposition," *Appl. Sci. Technol.*, vol. 10, no. 4, pp. 57–61, 2016.

[112] Q. Chen, "Research on high-performance receiving and rectifying technology for microwave wireless power transmission," Ph.D. dissertation, Sichuan Univ., 2020.

[113] L. Xiao, private communication, China Ship Develop. Design Ctr. (CSDDC), Wuhan, China.

[114] T. Takahashi *et al.*, "Phased array system for high efficiency and high accuracy microwave power transmission," in *Proc. IEEE MTT-S Int. Microw. Workshop Ser. Innov. Wireless Power Transmiss., Syst., Appl.*, May 12-13, 2011.

[115] S. Mihara *et al.*, "The plan of microwave power transmission development for SSPS and its industry application," in *Proc. Asia-Pacific Microw. Conf.*, 2018.

[116] "Space solar power dominates the D3 …is now the #1 idea in the federal government!" The Space Development Steering Committee, Apr. 3, 2016.

[117] K. Svitil, "Spaced-based solar power project funded," California Inst. Technol., Pasadena, CA, USA, Apr. 2015.

[118] E. E. Gdoutos *et al.*, "A lightweight tile structure integrating photovoltaic conversion and RF power transfer for space solar power applications," in *Proc. AIAA Spacecraft Structures Conf.*, Jan. 2018.

[119] M. Jorgenson, "Project directly supports the space solar power initiative converting solar power in space to radio frequency on earth," Northrop Grumman Newsroom, Dec. 11, 2019.

[120] M. Gal-Katziri, A. Fikes, F. Bohn, B. Abiri, M. R. Hashemi, and A. Hajimiri, "Scalable, deployable, flexible phased array sheets," in *Proc. IEEE Int. Microw. Symp.*, Aug. 2020, pp. 1458–1462.

[121] A. Fikes, A. Safaripour, F. Bohn, B. Abiri, and A. Hajimiri., "Flexible, conformal phased arrays with dynamic array shape self-calibration," in *Proc. IEEE Int. Microw. Symp.*, Jun. 2019, pp. 1085–1093.

[122] M. Gal-Katziri and A. Hajimiri, "Sub-picosecond hybrid DLL for large-scale phased array synchronization," in *Proc. IEEE Asian Solid-State Circuits Conf.*, Nov. 2018, pp. 231–236.

[123] [Online]. Available: https://www.spacesolar.caltech.edu

[124] "NRL conducts first test of solar power satellite hardware in orbit," U.S. Naval Res. Lab. Press Release, May 18, 2020.

[125] W. Brown, "Experiments in the transportation of energy by microwave beam," in *1958 IRE Int. Convention Rec.*, 1966.

[126] W. C. Brown and J. F. Triner, "Experimental thin-film, etched-circuit rectenna," *IEEE Int. Microw. Symp.*, 1982, pp. 185–187.

[127] J.-P. Curty, N. Joehl, C. Dehollain, and M. J. Declercq, "Remotely powered addressable UHF RFID integrated system," *IEEE J. Solid-State Circuits*, vol. 40, no. 11, pp. 2193–2202, Nov. 2005.

[128] W. Huang, B. Zhang, X. Chen, K.-M. Huang, and C.-J. Liu, "Study on an S-band rectenna array for wireless microwave power transmission," *Prog. Electromagn. Res.*, vol. 135, pp. 747–758, 2013.

[129] D.-J. Lee, S.-J. Lee, I.-J. Hwang, W.-S. Lee, and J.-W. Yu, "Hybrid power combining rectenna array for wide incident angle coverage in RF energy transfer," *IEEE Trans. Microw. Theory Techn.*, vol. 65, no. 9, pp. 3409–3418, Sept. 2017.

[130] U. Olgun, C.-C. Chen, and J. L. Volakis, "Wireless power harvesting with planar rectennas for 2.45 GHz RFIDs," in *Proc. URSI Int. Symp. Electromagn. Theory*, 2010.

[131] U. Olgun, C.-C. Chen, and J. L. Volakis, "Investigation of rectenna array configurations for enhanced RF power harvesting," *IEEE Antennas Wireless Propag. Lett.*, vol. 10, pp. 262–265, 2011.

[132] M. Roberg, T. Reveyrand, I. Ramos, E. A. Falkenstein, and Z. Popovic, "High-efficiency harmonically terminated diode and transistor rectifiers," *IEEE Trans. Microw. Theory Techn.*, vol. 60, no. 12, pp. 4043–4052, Dec. 2012.
[133] G. A. Vera, A. Georgiadis, A. Collado, and S. Via, "Design of a 2.45 GHz rectenna for electromagnetic (EM) energy scavenging," in *Proc. IEEE Radio Wireless Symp.*, 2010, pp. 61–64.
[134] Y.-H. Suh and K. Chang, "A high-efficiency dual-frequency rectenna for 2.45- and 5.8-GHz wireless power transmission," *IEEE Trans. Microw. Theory Techn.*, vol. 50, no. 7, pp. 1784–1789, Jul. 2002.
[135] W. C. Brown, "Electronic and mechanical improvement of the receiving terminal of a free-space microwave power transmission system," NASA Rep. NASA-CR-135194, Apr. 1977.
[136] W. C. Brown, "Rectenna technology program: Ultra light 2.45 GHz rectenna 20 GHz rectenna," NASA Rep. NASA-CR-179558, Mar. 1987.
[137] D. Wang and R. Negra, "Design of a dual-band rectifier for wireless power transmission," in *Proc. IEEE Wireless Power Transfer Conf.*, 2013, pp. 127–130.
[138] C.-H. K. Chin, Q. Xue, and C. H. Chan, "Design of a 5.8-GHz rectenna incorporating a new patch antenna," *IEEE Antennas Wireless Propag. Lett.*, vol. 4, pp. 175–178, 2005.
[139] M. C. Derbal and M. Nedil, "A high gain dual band rectenna for RF energy harvesting applications," *Prog. Electromagn. Res.*, vol. 90, pp. 29–36, 2020.
[140] M. Furukawa *et al.*, "5.8-GHz planar hybrid rectenna for wireless powered applications," *IEEE Asia-Pacific Microw. Conf*, 2006, pp. 1611–1614.
[141] S. Imai, S. Tamaru, K. Fujimori, M. Sanagi, and S. Nogi, "Efficiency and harmonics generation in microwave to DC conversion circuits of half-wave and full-wave rectifier types," in *Proc. IEEE Int. Microw. Workshop Ser. Innov. Wireless Power Transmiss., Technol., Syst., Appl.*, 2011, pp. 15–18.
[142] S. E. F. Mbombolo and C. W. Park, "An improved detector topology for a rectenna," in *Proc. IEEE Int. Microw. Workshop Ser. Innov. Wireless Power Transmiss., Technol., Syst., Appl.*, 2011, pp. 23–26.
[143] J. O. McSpadden, L. Fan, and K. Chang, "Design and experiments of a high-conversion-efficiency 5.8-GHz rectenna," *IEEE Trans. Microw. Theory Techn.*, vol. 46, no. 12, pp. 2053–2060, Dec. 1998.
[144] K. Nishida *et al.*, "5.8 GHz high sensitivity rectenna array," in *Proc. IEEE Int. Microw. Workshop Ser. Innov. Wireless Power Transmiss., Technol., Syst., Appl.*, 2011, pp. 19–22.
[145] T. Sakamoto, Y. Ushijima, E. Nishiyama, M. Aikawa, and I. Toyoda, "5.8-GHz series/parallel connected rectenna array using expandable differential rectenna units," *IEEE Trans. Antennas Propag.*, vol. 61, no. 9, pp. 4872–4875, Sep. 2013.
[146] B. Strassner and K. Chang, "Highly efficient C-band circularly polarized rectifying antenna array for wireless microwave power transmission," *IEEE Trans. Antennas Propag.*, vol. 51, no. 6, pp. 1347–1356, Jun. 2003.
[147] A. Kumar, "Antenna assists MW power transmission," *Semiconductors*, 2019.
[148] W. H. Tu, S. H. Hsu, and K. Chang, "Compact 5.8-GHz rectenna using stepped-impedance dipole antenna," *IEEE Antennas Wireless Propag. Lett.*, vol. 6, pp. 282–284, 2007.
[149] L. W. Epp, A. R. Khan, H. K. Smith, and R. P. Smith, "A compact dual-polarized 8.51-GHz rectenna for high-voltage (50 V) actuator applications," *IEEE Trans. Microw. Theory Techn.*, vol. 48, no. 1, pp. 111–120, Jan. 2000.
[150] Y. Kim, Y. J. Yoon, J. Shin, and J. So, "X-band printed rectenna design and experiment for wireless power transfer," in *Proc. IEEE Wireless Power Transfer Conf.*, 2014, pp. 292–295.
[151] M. Litchfield, S. Schafer, T. Reveyrand, and Z. Popović, "High-efficiency X-band MMIC GaN power amplifiers operating as rectifiers," in *Proc. IEEE Int. Microw. Symp.*, 2014, pp. 1–4.
[152] G. Monti, L. Tarricone, and M. Spartano, "X-band planar rectenna," *IEEE Antennas Wireless Propag. Lett.*, vol. 10, pp. 1116–1119, 2011.
[153] S. Schafer, M. Coffey, and Z. Popović, "X-band wireless power transfer with two-stage high-efficiency GaN PA/rectifier," in *Proc. IEEE Wireless Power Transfer Conf.*, 2015, pp. 1–3.
[154] J. Shin, M. Seo, J. Choi, J. So, and C. Cheon, "A compact and wideband circularly polarized rectenna with high efficiency at X-band," *Prog. Electromagn. Res.*, vol. 145, pp. 163–173, 2014.
[155] T.-W. Yoo and K. Chang, "Theoretical and experimental development of 10 and 35 GHz rectennas," *IEEE Trans. Microw. Theory Techn.*, vol. 40, no. 6, pp. 1259–1266, Jun. 1992.
[156] X. Yang, J.-S. Xu, and D.-M. Xu, "Compact circularly polarized rectennas for microwave power transmission applications," in *Proc. IEEE Int. Symp. Antennas Propag.*, 2006, pp. 1–4.
[157] K. Hatano, N. Shinohara, T. Seki, and M. Kawashima, "Development of MMIC rectenna at 24GHz," in *Proc. IEEE Radio Wireless Symp.*, 2013, pp. 199–201.
[158] N. Shinohara, K. Nishikawa, T. Seki, and K. Hiraga, "Development of 24 GHz rectennas for fixed wireless access," *URSI General Assembly Sci. Symp.*, 2011.
[159] A. Collado and A. Georgiadis, "24 GHz substrate integrated waveguide (SIW) rectenna for energy harvesting and wireless power transmission," in *Proc. IEEE Int. Microw. Symp.*, 2013, pp. 1–3.
[160] S. Ladan and K. Wu, "35 GHz harmonic harvesting rectifier for wireless power transmission," in *Proc. IEEE Int. Microw. Symp.*, 2014, pp. 1–4.
[161] P. Koert and J. T. Cha, "35 GHz rectenna development," in *Proc. IEEE Wireless Power Transmiss. Conf.*, 1993, pp. 1259–1266.
[162] T.-W. Yoo, "Experimental and theoretical study on 35 GHz rf-to-dc power conversion receiver for millimeter-wave beamed power transmission," Ph.D. dissertation, Dept. Elect. Eng., Texas A&M Univ., pp. 165, Dec. 1993.
[163] H.-K. Chiou and I.-S. Chen, "High-Efficiency dual-band on-chip rectenna for 35-and 94-GHz wireless power transmission in 0.13-μm CMOS technology," *IEEE Trans. Microw. Theory Techn.*, vol. 58, no. 12, pp. 3598–3606, Dec. 2010.
[164] S. Hemour, C. H. P. Lorenz, and K. Wu, "Small-footprint wideband 94GHz rectifier for swarm micro-robotics," in *Proc. IEEE Int. Microw. Symp.*, 2015, pp. 1–4.
[165] P. He and D. Zhao, "A W-Band switching rectifier with 27% efficiency for wireless power transfer in 65-nm CMOS," in *Proc. IEEE Int. Microw. Symp.*, 2019, pp. 634–637.
[166] N. Weissman, S. Jameson, and E. Socher, "W-band CMOS on-chip energy harvester and rectenna," in *Proc. IEEE Int. Microw. Symp.*, 2014, pp. 1–3.
[167] A. D. Vroede, S. Ooms, B. Philippe, and P. Reynaert, "A 94 GHz voltage-boosted energy harvester in 45 nm CMOS achieving a peak efficiency of 21.2% at -8.5 dBm input power," in *Proc. IEEE EUROCON 18th Int. Conf. Smart Technol.*, 2019.
[168] K. Matsui *et al.*, "Microstrip antenna and rectifier for wireless power transfer at 94GHz," in *Proc. IEEE Wireless Power Transfer Conf.*, 2017, pp. 1–3.
[169] A. Etinger *et al.*, "Characterization of a Schottky diode rectenna for millimeter wave power beaming using high power radiation sources," *Acta Physica Polonica A*, vol. 131, pp. 1280–1284, 2017.
[170] E. Shaulov, S. Jameson, and E. Socher, "W-band energy harvesting rectenna array in 65-nm CMOS," in *Proc. IEEE Int. Microw. Symp.*, 2017, pp. 307–310.
[171] R. H. George, "Solid-state power rectifications," *Microw. Power Eng.*, vol. 1, pp. 275–294, 1968.
[172] W. C. Brown, R. H. George, N. I. Heenan, and R. C. Wonson, "Microwave to DC converter," U.S. Patent 3,434,678, 1969.
[173] R. M. Dickinson, "Evaluation of a microwave high-power reception-conversion array for wireless power transmission," NASA JPL Tech. Memo., pp. 33–741, Sep. 1, 1975.
[174] R. M. Dickinson and W. C. Brown, "Radiated microwave power transmission system efficiency measurements," Tech. Memo. 33-727, Jet Propulsion Lab., California Inst. Technol., Mar. 15, 1975.
[175] W. C. Brown and J. F. Triner, "Experimental thin-film, etched-circuit rectenna," in *IEEE MTT-S Dig.*, 1982.
[176] J. Schlesak, A. Alden, and T. Ohno, "SHARP rectenna and low altitude flight trials," in *Proc. IEEE Glob. Telecommun. Conf.*, New Orleans, Dec. 2–5, 1985, pp. 283–228.
[177] Y. Fujino *et al.*, "A rectenna for MILAX," in *Proc. Wireless Power Transmiss. Conf.*, Feb. 1993, pp. 273–277.
[178] N. Kaya, S. Ida, Y. Fujino, and M. Fujita, "Transmitting antenna system for airship demonstration (ETHER)," *Space Energy Transp.*, vol. 1, no. 4, pp. 237–245, 1996.
[179] B. Strassner and K. Chang, "Highly efficient C-band circularly polarized rectifying antenna array for wireless microwave power transmission," *IEEE Trans. Antennas Propag.*, vol. 51, no. 6, pp. 1347–1356, Jun. 2003.

[180] R. Andryczyk, P. Foldes, J. Chestek, and B. Kaupang, "Solar power satellite ground stations," *IEEE Spectr.*, vol. 16, no. 7, pp. 51–55, Jul. 1979.
[181] J. Hagerty and Z. Popović, "An experimental and theoretical characterization of a broadband arbitrarily-polarized rectenna array," in *IEEE MTT-S Int. Microw. Symp. Dig.*, May 2001, pp. 1855–1858.
[182] W. Huang, B. Zhang, X. Chen, K. Huang, and C. Liu, "Study on an S-Band rectenna array for wireless microwave power transmission," *PIERS*, vol. 135, pp. 747–758, 2013.
[183] H. Takhedmit, L. Cirio, F. Costa, and O. Picon, "Transparent rectenna and rectenna array for RF energy harvesting at 2.45 GHz," in *Proc. 8th EuCAP*, 2014.
[184] B. Zhanga *et al.*, "Experimental study on an S-band nearfield microwave magnetron power transmission system on hundred-watt level," *Int. J. Electron.*, Jan. 7, 2015.
[185] E. Shaulov, S. Jameson, and E. Socher, "W-band energy harvesting rectenna array in 65-nm CMOS," in *Proc. IEEE-MTT-S IMS*, Jun. 4–9, 2017, pp. 307–310.
[186] A. Ashoor, T. Almoneef, and O. Ramahi, "A planar dipole array surface for electromagnetic energy harvesting and wireless power transfer," *IEEE Trans. Microwave Theory Techn.*, vol. 66, no. 3, pp. 1553–1560, Mar. 2018.
[187] Y. Park, K. Kim, and D. Youn, "Rectenna array design for receiving high power in bea type wireless power transmission," in *Proc. Asia-Pacific Microw. Conf.*, 2018.
[188] W. Huang, J. Du, G. Tan, and X. Yang, "A novel 35-GHz slot-coupled patch rectenna array based on SIW cavity for WPT," in *Proc. ICMMT*, May 19–22, 2019.
[189] P. Jaffe and J. McSpadden, "Energy conversion and transmission modules for space solar power," *Proc. IEEE*, vol. 101, no. 6, pp. 1424–1437, Jun. 2013.
[190] P. Jaffe, "A Sunlight-to-microwave power transmission module prototype for space solar power," M.S. thesis, Dept. Elect. Comput. Eng., Univ. Maryland, College Park, MD, USA, 2013.
[191] S. LeVine, "The active denial system: A revolutionary, non-lethal weapon for today's battlefield," Ctr. Technol. Nat. Security Policy, Nat. Defense Univ., Jun. 2009.
[192] B. Danly *et al.*, "Development and testing of a high-average power, 94-GHz gyroklystron," *IEEE Trans. Plasma Sci.*, vol. 28, no. 3, pp. 713–726, Jun. 2000.
[193] E. Robinson, "Solid state active denial technology demonstrator program," in *Proc. Joint Armaments Conf.*, May 2012.
[194] K. Brown *et al.*, "7kW GaN W-band transmitter," in *Proc. IEEE Int. Microw. Symp.*, 2016, pp. 1–3.
[195] H. Kazemi, K. Shinohara, and C. W. Eckhardt, "Millimeter wave wireless power transmission- Technologies and applications," in *Proc. IEEE IWPC*, 2019, pp. 282–286.
[196] *Manual of Regulations and Procedures for Federal Radio Frequency Management*, Sep. 2017 Revision of the May 2013 Edition, NTIA, [Online]. 2017. Available: https://www.ntia.doc.gov/page/2011/manual-regulations-and-procedures-federal-radio-frequency-management-redbook
[197] "Satellite power system concept development and evaluation program, reference system report," Rep. DOE/ER-0023, Oct. 1978.
[198] H. P. Davis, "Space-based solar power, an update," Solar High Study Group, Aug. 23rd, 2012.
[199] *IEEE Standard for Safety Levels with Respect to Human Exposure to Electric, Magnetic, and Electromagnetic Fields, 0 Hz to 300 GHz*," IEEE Std C95.1-2019, Oct. 2019.
[200] "ANSI Z136 standards," The Laser Institute, Aug. 11, 2017. Accessed: Jun. 25, 2020. [Online]. Available: https://www.lia.org/resources/laser-safety-information/laser-safety-standards/ansi-z136-standards
[201] "ICNIRP guidelines for limiting exposure to electromagnetic fields (100 kHz to 300 GHz)," *Health Phys*, vol. 118, no. 5, pp. 483–524, Mar. 2020.
[202] T. J. Nugent, Jr., D. Bashford, T. Bashford, T. J. Sayles, and A. Hay, "Long-range, integrated, safe laser power beaming demonstration," in *Opt. Wireless Fiber Power Transmiss. Conf. (OWPT) Tech. Dig.*, Apr. 2020, pp. 12–13.
[203] P. Jaffe *et al.*, "Opportunities and challenges for space solar for remote installations," NRL Rep. MR-8243-19-9813, Oct. 2019.

CHRISTOPHER T. RODENBECK (Senior Member, IEEE) received the B.S. (*summa cum laude*), M.S., and Ph.D. degrees in electrical engineering from Texas A&M University, College Station, TX, USA, in 1999, 2001, and 2004, respectively. His graduate studies were supported by fellowships from NASA, the State of Texas "to advance the state of the art in telecommunications," Texas A&M, and TxTEC in addition to grants from Raytheon, TriQuint Semiconductor, the Office of the Secretary of Defense, NASA Jet Propulsion Lab, NASA Glenn Research Center, and the US Army Space Command.

He is currently an Office Head with U.S. Naval Research Laboratory in Washington, DC, where he leads the Radar Division's Advanced Concepts Group and is responsible for multiple research programs in millimeter-wave airborne radar and advanced electronics. From 2004 to 2014, he led a multidisciplinary advanced/exploratory technology development program for radar and sensor applications at Sandia National Laboratories in Albuquerque, NM. The success of this work was twice the subject of Congressional testimony by Sandia's President. He has mentor numerous engineers in the radar electronics application area. He has authored or coauthored 40 refereed journal papers, 22 patents and patent applications, 29 conference papers, and 29 government reports. He is responsible for numerous radar technology innovations in short- and long-range airborne millimeter wave radar systems and antennas, ultrawideband pulsed power amplifiers, CMOS radiation hardening by design, highly sensitive radar digitizers, advanced RF modules, electro-optical inspection of RF circuits, solid-state device modeling, electrically small antennas, and software-defined fusion of radar and telemetry. He is a Principal Investigator on multiple ongoing power beaming programs at NRL. Dr. Rodenbeck was the recipient of the 2016 Texas A&M University Outstanding Early Career Professional Achievement Award from among more than 100,000 engineering alumni. He received the IEEE MTT-S Outstanding Young Engineer Award in 2015, was the Principal Investigator for an R&D program receiving the prestigious 2012 NNSA Award of Excellence, received a Sandia Innovator Award in 2013, and was awarded an internal citation for "Excellence in Radar Technology Leadership" in 2011. He was an Associate Editor of the *Encyclopedia of Electrical and Electronics Engineering* (New York, NY, USA: Wiley) from 2011 to 2020, and currently is the Editor-in-Chief of the *Encyclopedia of RF & Microwave Engineering, 2nd ed.* (New York, NY, USA: Wiley).

PAUL I. JAFFE (Senior Member, IEEE) received the B.S. degree from the University of Maryland, College Park, MD, USA, in 1996 and the M.S. degree from the Johns Hopkins University, Baltimore, MD, USA, in 2007, graduating with honors. He also received the Ph.D. degree from the University of Maryland, College Park in 2013, all in electrical engineering.

He is an Electronics Engineer and Researcher with the U.S. Naval Research Laboratory, Washington, DC, USA. In the past 25 years, he has worked on over two dozen space missions, often as the principal investigator. He was a Coordinator and Editor for two NRL-led space solar power reports, one published in 2009 and the other in 2019. He has managed large, multidisciplinary teams as the Electrical Segment Lead for several critical space programs and overseen a portfolio of power beaming and space solar projects. His research interests include power beaming, novel space systems and technologies, renewable energy sources, and efficacy in K-12 Science, Technology, Engineering, and Mathematics (STEM) education. He has authored or coauthored more than fifty technical publications and holds a U.S. patent, with others pending. He was the author of the space solar chapter in the third edition of *Future Energy*, and he has made numerous appearances in international television, radio, print, and online media as a subject matter expert on space solar and power beaming, including as a TEDx speaker.

Dr. Jaffe has thrice been the recipient of the Alan Berman Research Publication Award. He received the Vice Admiral Samuel L. Gravely, Jr., STEM and Diversity Champion of the year award for 2012. In 2015, he was named a recipient of the Institute of Environmental Sciences and Technology's Maurice Simpson Technical Editors Award. In 2016, he led a team to win most of the awards in the Secretary of Defense-sponsored Defense, Diplomacy, and Development (D3) Innovation Summit Pitch Challenge, those for: Innovation, Presentation, Collaboration, and People's Choice. He served on the technical committee of the International SpaceWire Conference and was a session organizer for several years of the IEEE Aerospace Conference.

BERND H. STRASSNER II received the B.S. degree in electrical engineering from the Rose-Hulman Institute of Technology, Terre Haute, IN, in 1995, and the M.S. and Ph.D. degrees in electrical engineering from Texas A&M University, College Station, in 1997 and 2002, respectively.

Since July 2002, he has been with Sandia National Laboratories, Albuquerque, NM, where he designs a variety of wideband antenna arrays for synthetic aperture radar and communication systems. From 1998 to 2002, he was a Research Assistant with Texas A&M University's Electromagnetics Laboratory, where his research focused on passive-backscatter RFID tags for tracking pipe in oil drill strings, rectifying antenna arrays for microwave power reception, and reflecting antenna arrays for space platforms. From 1996 to 1997, he was with Sandia National Laboratories, Albuquerque, NM, where he was involved with the study on how harmonic load-pull terminations affect power-amplifier performance.

PAUL E. HAUSGEN received the B.S. degree in mechanical engineering from Louisiana Tech University, Ruston, LA, USA, in 1993, graduating with honors (*summa cum laude*). In 1993, he was selected for the Air Force Palace Knight graduate intern program, which funded his graduate education and research. In 1994, he received the M.S. degree in mechanical engineering from the Georgia Institute of Technology, Atlanta, GA, USA. After conducting research in thermal-to-electric energy conversion technologies for the Air Force Phillips Laboratory, he returned to the Georgia Institute of Technology in 1996 and was awarded a Ph.D. in mechanical engineering in 2000.

He is currently a Senior Research Mechanical Engineer with the Air Force Research Laboratory, Space Vehicles Directorate, and is a civilian member of the newly commissioned United States Space Force. He is dual-hatted as the Deputy Branch Chief for the Spacecraft Component Technology Branch and as the Principal Investigator for the Space Solar Power Incremental Demonstrations and Research Project (SSPIDR). He has over 20 years of experience researching and leading teams of researchers in technology development for spacecraft to include space power, thermal, structures, electronics, guidance navigation and control, and decision support systems. He has led spacecraft power technology flight experiments that include the Experimental Solar Array on the Air Force Research Laboratory's TacSat 2 spacecraft and multiple experiments on the International Space Station.

Dr. Hausgen holds one U.S. patent in spacecraft power technology, and one pending patent in the area of spacecraft-to-spacecraft power beaming. He has authored or coauthored more than 34 research publications and one book chapter in spacecraft power related technologies. He has received multiple awards for R&D in spacecraft technology development that include a team RNASA Stellar Award in 2018, an R&D 100 team award in 2016, the Federal Laboratory Consortium Excellence in Tech Transfer in 2016, and the Air Force Civilian Achievement Award in 2013.

JAMES O. McSPADDEN (Senior Member, IEEE) received the B.S.E.E, M.S.E.E and Ph.D. degrees, from Texas A&M University, in 1989, 1993, and 1998, respectively.

He is an expert in microwave power transmission systems and rectenna design. Working for over 20 years in industry, he has led projects performing system analysis and technology development for various power transmission projects. He has been a Raytheon Technologies consultant on power beaming studies for the DoD, DARPA, NASA, universities, and private companies.

Dr. McSpadden has 30 presentations and published papers in journals, conferences, and magazines on microwave power transmission.

HOOMAN KAZEMI (Senior Member, IEEE) received the B.S, M.S and Ph.D. degrees from Department of Electrical and Electronic Engineering, University of Leeds, U.K. He is an Engineering Fellow with Raytheon Technologies in the Intelligence and Space System business unit. He is part of the advanced concepts and technology systems department and focus on developing advanced microwave and millimeter wave technologies. His research interests include high power directed energy portfolio systems including high power transmitters and high sensitivity receivers to provide new capabilities such as non-lethal repel effects, advanced biometrics, see thru clothing imaging. Another area of work has been high data rate communication using millimeter wave frequency range for multi-Gbps links on moving platforms towards ultra-low size weight and power (SWAP) systems. His recent focus is on developing millimeter wave wireless power systems including high power sources and high efficiency receivers delivering power at long range for a variety of applications. He currently developing high power Rectenna circuits and systems together with a variety of sources to enable stand-off wireless power beaming in various modalities of ground, air and space. He has published numerously and in receipt of multiple patents in the areas discussed.

NAOKI SHINOHARA (Senior Member, IEEE) received the B.E. degree in electronic engineering and the M.E. and Ph.D. (Eng.) degrees in electrical engineering from Kyoto University, Kyoto, Japan, in 1991, 1993, and 1996, respectively.

He has been a Research Associate with the Radio Atmospheric Science Center, Kyoto University, since 1996. He has been a Research Associate with the Radio Science Center for Space and Atmosphere, Kyoto University, by recognizing the Radio Atmospheric Science Center, since 2000, where he has been an Associate Professor since 2001. He has been an Associate Professor with the Research Institute for Sustainable Humanosphere, Kyoto University, by recognizing the Radio Science Center for Space and Atmosphere, since 2004. Since 2010, he has been a Professor with the Research Institute for Sustainable Humanosphere, Kyoto University. He has been engaged in research on solar power station/satellite and microwave power transmission systems.

Prof. Shinohara is an IEEE Distinguish Microwave Lecturer, the IEEE MTT-S Technical Committee 26 (Wireless Power Transfer and Conversion) Vice Chair, the IEEE MTT-S Kansai Chapter TPC Member, the IEEE Wireless Power Transfer Conference Advisory Committee Member, the *International Journal of Wireless Power Transfer* (Cambridge Press) Executive Editor, the Radio Science for URSI Japanese Committee C Member, the Past Technical Committee Chair on the IEICE Wireless Power Transfer, the Japan Society of Electromagnetic Wave Energy Applications Vice Chair, the Wireless Power Transfer Consortium for Practical Applications (WiPoT) Chair, and the Wireless Power Management Consortium (WPMc) Chair.

BRIAN B. TIERNEY (Member, IEEE) received the B.S. degree in electrical engineering from Kansas State University, Manhattan, KS, USA, in 2011 and the M.S.E and Ph.D. degrees in electrical engineering from the University of Michigan, Ann Arbor, Ann Arbor, MI, USA, in 2014 and 2016, respectively

Since 2016, he has been with the Radar Division of the U.S. Naval Research Laboratory in Washington, DC, USA. His current research interests include advanced radar concepts, microwave circuits, wireless power transfer, electromagnetic theory, and digital signal processing.

CHRISTOPHER B. DePUMA is an Electronics Engineer with the Spacecraft Electronics branch of the U.S. Naval Research Laboratory (NRL), where he is the Program Manager for the Photovoltaic Radiofrequency Antenna Module (PRAM). This experiment, currently flying on the Air Force X-37B, is a prototype of a future Solar Power Satellite that aims to convert solar energy in space to a microwave transmission that can be sent back to earth for terrestrial use. He has also supported the DARPA-funded, NRL-led Robotic Servicing of Geosynchronous Satellites (RSGS) program on tasks including the environmental test campaign and harness design efforts. In addition to the previously mentioned space efforts, Mr. DePuma leads demonstration activities for the Safe and Continuous Power Beaming – Microwave (SCOPE-M) program.

AMANDA P. SELF received the B.S. and M.S. degrees in aerospace engineering from the Georgia Institute of Technology, Atlanta, GA, USA in 2009 and 2012.

She is currently the Chief Engineer of the SSPIDR Program. Since 2011, she has been with the Air Force Research Laboratory, both as a contractor and civilian, in the Space Vehicles Directorate. She served as the Lead Mission Planner for the EAGLE spacecraft (launched in Apr. 2018) and executed the first successful deployment of an ESPA-Class satellite from a propulsive ESPA bus as well as coordinated the execution of mission objectives for EAGLE's nine different payloads during experimental and high-tempo on-orbit operations. From 2011 to 2016, he was the Lead Systems Engineer of the AFRL's University Nanosat Program (UNP)—a program created to lead students through the entire satellite process from cradle to grave. While working on UNP, she was SME for over forty universities as they developed and built satellite programs, integrated and tested ten small satellites, and saw four of those satellites through the operations phase.